AD-A102 268 SYRACUSE UNIV NY F/6 9/5
TIME-DOMAIN IN ANALYSIS OF LUMPED/DISTRIBUTED NETWORKS FOR ELEC--ETC(U)
JUN 81 J L ALLEN F30602-79-C-0011
UNCLASSIFIED RADC-TR-81-110 NL

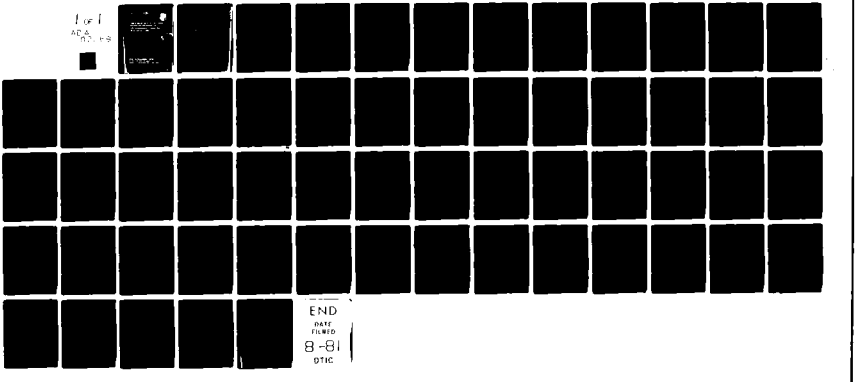

END
DATE FILMED
8-81
DTIC

RADC-TR-81-110
Phase Report
June 1981

LEVEL II

12

TIME-DOMAIN ANALYSIS OF LUMPED/ DISTRIBUTED NETWORKS FOR ELECTROMAGNETIC COMPATIBILITY (ECM) APPLICATIONS

University of South Florida

J. Lamar Allen

ROME AIR DEVELOPMENT CENTER
Air Force Systems Command
Griffiss Air Force Base, New York 13441

This report has been reviewed by the RADC Public Affairs Office (PA) and is releasable to the National Technical Information Service (NTIS). At NTIS it will be releasable to the general public, including foreign nations.

RADC-TR-81-110 has been reviewed and is approved for publication.

APPROVED: Roy F. Stratton

ROY F. STRATTON
Project Engineer

APPROVED: David C. Luke

DAVID C. LUKE, Colonel, USAF
Chief, Reliability & Compatibility Division

FOR THE COMMANDER: John P. Huss

JOHN P. HUSS
Acting Chief, Plans Office

If your address has changed or if you wish to be removed from the RADC mailing list, or if the addressee is no longer employed by your organization, please notify RADC (RBCT) Griffiss AFB NY 13441. This will assist us in maintaining a current mailing list.

Do not return this copy. Retain or destroy.

ERRATA

29 July 1981

RADC-TR-81-110 dated June 1981

TIME-DOMAIN ANALYSIS OF LUMPED/DISTRIBUTED NETWORKS FOR ELECTROMAGNETIC COMPATIBILITY (ECM) APPLICATIONS

The title on the cover and in Block 4 of the DD Form 1473 should be corrected to read:

TIME-DOMAIN IN ANALYSIS OF LUMPED/DISTRIBUTED NETWORKS FOR ELECTROMAGNETIC COMPATIBILITY (EMC) APPLICATIONS.

Rome Air Development Center
Air Force Systems Command
Griffiss Air Force Base, New York 13441

UNCLASSIFIED

SECURITY CLASSIFICATION OF THIS PAGE (When Data Entered)

REPORT DOCUMENTATION PAGE	READ INSTRUCTIONS BEFORE COMPLETING FORM
1. REPORT NUMBER: RADC-TR-81-110 ✓	2. GOVT ACCESSION NO.: AD-A102268
3. RECIPIENT'S CATALOG NUMBER	
4. TITLE (and Subtitle): TIME-DOMAIN ANALYSIS OF LUMPED/DISTRIBUTED NETWORKS FOR ELECTROMAGNETIC COMPATIBILITY (ECM) APPLICATIONS.	5. TYPE OF REPORT & PERIOD COVERED: Phase Report. Jun 79 — Aug 80.
	6. PERFORMING ORG. REPORT NUMBER: N/A
7. AUTHOR(s): J. Lamar Allen	8. CONTRACT OR GRANT NUMBER(s): F30602-79-C-0011 ✓
9. PERFORMING ORGANIZATION NAME AND ADDRESS: Syracuse University, Syracuse NY 13210	10. PROGRAM ELEMENT, PROJECT, TASK AREA & WORK UNIT NUMBERS: 62702F, 23380317, 03
11. CONTROLLING OFFICE NAME AND ADDRESS: Rome Air Development Center (RBCT), Griffiss AFB NY 13441	12. REPORT DATE: Jun 81; 57
	13. NUMBER OF PAGES: 59
14. MONITORING AGENCY NAME & ADDRESS (if different from Controlling Office): Same	15. SECURITY CLASS. (of this report): UNCLASSIFIED
	15a. DECLASSIFICATION/DOWNGRADING SCHEDULE: N/A

16. DISTRIBUTION STATEMENT (of this Report)
Approved for public release; distribution unlimited.

17. DISTRIBUTION STATEMENT (of the abstract entered in Block 20, if different from Report)
Same

18. SUPPLEMENTARY NOTES
RADC Project Engineer: Roy F. Stratton

19. KEY WORDS (Continue on reverse side if necessary and identify by block number)
Time-Domain Analysis
Distributed Circuits
Y Matrix Approach
Transmission
Line Analysis
Models

20. ABSTRACT (Continue on reverse side if necessary and identify by block number)
A new technique suitable for time-domain analysis of a very general class of lumped/distributed networks is introduced. The basic procedure is described and illustrated with examples. The analysis procedure can also be used to generate time-domain models of transmission lines and other structures. This feature is illustrated by generating an exceptionally simple model for lossless transmission lines. Finally, a novel concept using time-varying reflection coefficients is introduced.

DD FORM 1 JAN 73 1473 EDITION OF 1 NOV 65 IS OBSOLETE

UNCLASSIFIED

SECURITY CLASSIFICATION OF THIS PAGE (When Data Entered)

TIME-DOMAIN ANALYSIS OF LUMPED/DISTRIBUTED NETWORKS FOR EMC APPLICATIONS

1.0 INTRODUCTION

Time-domain analysis of electronic networks, which deliberately or inadvertently incorporate transmission lines and other distributed elements, is increasingly important in EMC applications. Digital systems used for control, communications and computation must routinely process high speed pulses. Lightning, EMP and various other effects can induce unwanted pulses into both analog and digital systems. Compatibility analysis requires the ability to treat pulses in such systems under both normal and abnormal conditions. Shielding requirements and/or potential interference levels must be evaluated. Coupled transmission lines, branched cable bundles, and other complex combinations of wires frequently occur. Transmission lines can also be used to model a variety of electromagnetic shields.

The purpose of this report is to introduce and describe a new technique [1] suitable for the time-domain analysis of a very general class of lumped, distributed networks. An incidental but powerful feature of the new technique is that the same system equation formulation procedure yields either time-domain or frequency-domain equations. Considerable saving results when both frequency and time solutions are to be obtained. In the current report the basic procedure is described and illustrated with examples. The analysis procedure can also be used to generate time-domain models of transmission lines and other complex structures. This feature is illustrated by generating an exceptionally simple model for lossless transmission lines. Finally, a novel concept using time-varying reflection coefficients is introduced.

It should be emphasized that the procedure to be described is very general and applicable to a broad class of problems. Further applications and in particular time-domain models for lossy transmission lines and coupled line structures will be covered in future reports.

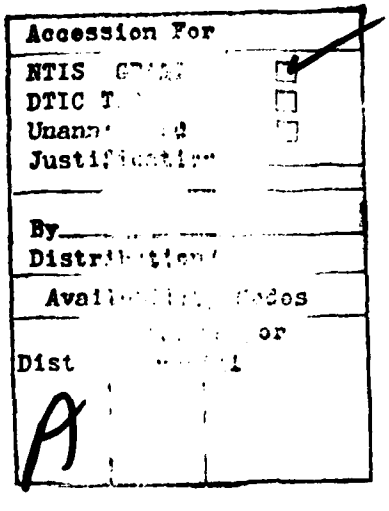

2.0 TIME-DOMAIN ANALYSIS OF LUMPED/DISTRIBUTED NETWORKS

Time-domain analysis of lumped element networks is well established. Powerful analytical and numerical technqiues are readily available, including the popular state-space and Laplace-transform methods. General purpose computer programs such as SCEPTRE [2] and SPICE [3] provide easy-to-implement time-domain solutions for complex lumped systems even when nonlinear, time-varying, and/or active elements are included.

The development of methods for transient analysis of mixed lumped-distributed networks is of relatively recent origin, and general techniques that permit, for example, lossy transmission lines of arbitrary lengths and nonlinear active lumped elements are not yet available. Yet, as pointed out above, the time-domain analysis of such networks is increasingly important in EMC analysis and prediction as well as normal design considerations for a variety of pulse processing systems inlcuded in communications, control, computing and radar applications. The technique to be described is widely applicable to the analysis of such systems.

During the course of this study, a substantial literature search was carried out. The most pertinent articles and books are listed for the reader's convenience [4-18]. While the technique to be presented is significantly different from the methods found in the literature, the present concept grew from "wouldn't it be nice if ••••" considerations following a reading of Silverberg's [4] paper. The new technique has been successfully applied to a wide variety of problems. The impact of Silverberg's work is gratefully acknowledged.

2.1 SYSTEM EQUATION FORMULATION: Part I

Assume that the system for EMC analysis has a network model consisting of interconnections of linear distributed elements, dependent sources, and

independent sources. Partition the network into two parts as shown in Figure 1. One part consists of linear (distributed and/or lumped) elements. The other part contains any lumped nonlinear or time-varying elements and independent sources.

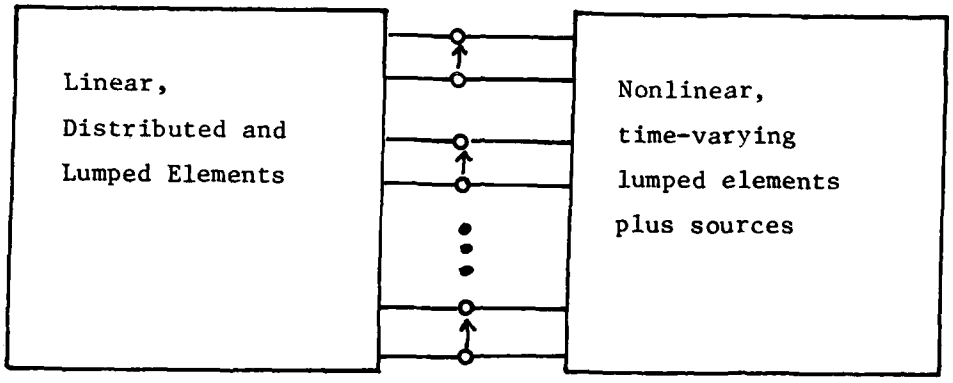

Figure 1. Partitioned network

Silverberg's [4] procedure is to solve for the terminal behavior of the linear part of the network in the frequency domain and then convert to a terminal time domain description by numerical inverse transform techniques. The time domain solution for the whole network is obtained step by step in time at the interface of the two parts by simultaneous solution of a convolution equation representing the linear part and a differential equation representing the nonlinear part. The simultaneous solution is accomplished at each time increment by solving algebraic equations obtained by application of the trapezoidal integration rule to the original equations.

For the moment let us focus our attention on the linear part of the network. Wouldn't it be nice if the frequency domain calculations and the inverse transform calculations could be eliminated and all calculations be performed directly in the time domain? Computer program complexity, memory requirements, and computational time could all be significantly reduced. The catch is that we would need a way of combining element descriptions to form network

descriptions such that the resulting network matrix is directly compatible with convolution solutions. Basically this implies that the overall system matrix should contain only sums or differences of individual element responses (no products or quotients allowed). The indefinite admittance matrix [19] appeared a good possibility, but because of the type of systems to be considered, a port-description method rather than a terminal description method was desired. Kron's transformation methods [20] provided the inspiration for the technique to be described. Ultimately, it became clear that for the present requirements, the formal transformation techniques could be replaced by a very simple algorithm. The more general Kron's method is first presented and then the revised and simplified algorithm is introduced via examples.

At this point, the problem statement for the linear part of the network is the following. Determine a scheme for representing networks such that given the terminal step-response of the subnetworks (or elements) in the time domain, the time-domain terminal step-response for the connected overall network can be determined as sums and differences of the individual subnetwork responses. Then by convolution the time-domain terminal response of the overall network can be determined for any specified set of inputs.

2.1.1 Kron's Method

Short-circuit admittance parameters will be used. A dual impedance formulation has also been used successfully. Following Kron [20], let

$$\vec{I} = \overleftrightarrow{Y}\vec{V}$$

be the given matrix equation for a network, where $\vec{I}$ is the current vector, $\vec{V}$ is the voltage vector, and $\overleftrightarrow{Y}$ is the admittance matrix. Suppose a new matrix equation $\vec{I}' = \overleftrightarrow{Y}'\vec{V}'$ is desired for the given network, where $\vec{I}'$, $\vec{V}'$, and $\overleftrightarrow{Y}'$ are the new current, voltage and admittance quantities, respectfully. Let the relationship between the old and new voltage quantities be

$$\vec{V} = \overleftrightarrow{C}\vec{V}'$$

where $\overleftrightarrow{C}$ is the voltage transformation matrix. In most cases the elements of $\overleftrightarrow{C}$ will be 1's and 0's.

Power in the network must be the same for either choice of variables, since the network is in no way changed by the change of variables. Thus,

$$\vec{V}_t^{*}\vec{I} = \vec{V}_t'^{*}\vec{I}'$$

must be true where subscript "t" indicates "matrix transpose" and superscript "*" indicates "complex conjugate." Substituting $\vec{V} = \overleftrightarrow{C}\vec{V}'$ yields

$$\vec{V}_t'^{*}\overleftrightarrow{C}_t^{*}\vec{I} = \vec{V}_t'^{*}\vec{I}'$$

so that

$$\vec{I}' = \overleftrightarrow{C}_t^{*}\vec{I}$$

and

$$\overleftrightarrow{Y}' = \overleftrightarrow{C}_t^{*}\overleftrightarrow{Y}\overleftrightarrow{C}$$

Collecting the above results yields the necessary relationships between old and new network quantities. Associating the "old" (unprimed) quantities with the disconnected subnetworks and the "new" (primed) quantities with the interconnected subnetworks leads to an algorithm for generating the system equations. The pertinent equations are given below.

First establish the relationship between the "new" and "old" voltage quantities to generate the transformation matrix, $\overleftrightarrow{C}$.

$$\vec{V} = \overleftrightarrow{C}\vec{V}' \qquad \text{(I)}$$

Next determine the "new" admittance matrix from the "old" admittance matrix and the transformation matrix obtained from Equation I.

$$\overleftrightarrow{Y}' = \overleftrightarrow{C}_t^{*}\overleftrightarrow{Y}\overleftrightarrow{C} \qquad \text{(II)}$$

The "new" system equation can then be written.

$$\vec{I}' = \overleftrightarrow{Y}'\vec{V}' \qquad \text{(III)}$$

The "new" currents can be related to the "old" currents and the transformation matrix.

$$\vec{I}' = \vec{C}_t^{*}\vec{I} \qquad \text{(IV)}$$

This procedure is best understood through examples.

2.1.2 Combining Subnetworks/Simplified Method

Initially Kron's method is used. However, it will be shown that the constraint of allowing only addition or subtraction of subnetwork matrix elements leads to a simple algorithm that eliminate a number of steps from Kron's procedure. The underlying feature of the simplified method is to treat every kind of connection as though it is a parallel connection. This approach requires that open-circuited ports be added to the network in certain situations. Such additional ports are like ideal voltmeter connections enabling determination of voltage at that point in the network without disturbing the system. The added open-circuited ports increase the size of the system matrix but the associated currents are zero and the overall system matrix is sparse. The net effect of this type of transformation on computational efficiency has thus far seemed to be increased efficiency. The following examples illustrate the conversion from Kron's method to the simplified algorithm.

2.1.2.1 Example 1

Given the 2-port networks "A" and "B," each represented by its admittance matrix as shown in Figure 2a, create a 3-port network by connecting ports 1 and 3 in parallel as shown in Figure 2b. Determine the admittance matrix of the 3-port in terms of the original unconnected 2-ports.

Following Kron's method, first generate the "primitive" admittance matrix for the unconnected subnetworks.

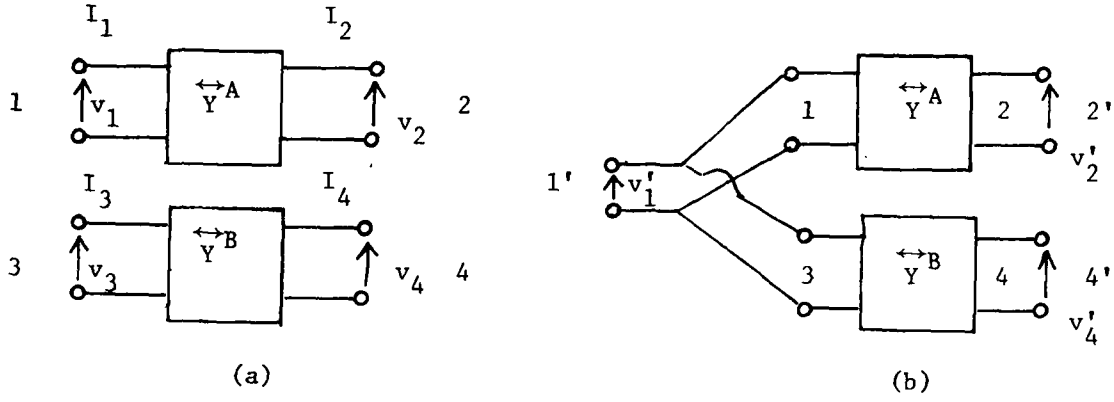

Figure 2.a) Two unconnected 3-ports
b) 2-ports "A" and "B" interconnected to form a 3-port

$$\overleftrightarrow{Y}_{SUB} = \begin{array}{c|cccc} & 1 & 2 & 3 & 4 \\ \hline 1 & Y^A_{11} & Y^A_{12} & 0 & 0 \\ 2 & Y^A_{21} & Y^A_{22} & 0 & 0 \\ 3 & 0 & 0 & Y^B_{11} & Y^B_{12} \\ 4 & 0 & 0 & Y^B_{21} & Y^B_{22} \end{array} \qquad (1)$$

Next the connection matrix relating "old" to "new" voltage variables is generated as in Equation I.

$$\vec{v}_{old} = \overleftrightarrow{C}\,\vec{v}_{new} \tag{2}$$

$$\begin{array}{|c|} \hline v_1 \\ \hline v_2 \\ \hline v_3 \\ \hline v_4 \\ \hline \end{array} = \begin{array}{c|ccc} & 1' & 2' & 3' \\ \hline 1 & 1 & 0 & 0 \\ 2 & 0 & 1 & 0 \\ 3 & 1 & 0 & 0 \\ 4 & 0 & 0 & 1 \end{array} \begin{array}{|c|} \hline v_1' \\ \hline v_2' \\ \hline v_4' \\ \hline \end{array} \tag{3}$$

Now the 3-port admittance matrix can be determined using Equation II.

$$\overleftrightarrow{Y}_{3\text{-Port}} = \overleftrightarrow{C}_t^{*}\,\overleftrightarrow{Y}_{SUB}\,\overleftrightarrow{C} \tag{4}$$

$$\overleftrightarrow{Y}_{3\text{-Port}} = \begin{array}{c|cccc} & 1 & 2 & 3 & 4 \\ \hline 1' & 1 & 0 & 1 & 0 \\ 2' & 0 & 1 & 0 & 0 \\ 4' & 0 & 0 & 0 & 1 \end{array} \begin{array}{c|cccc} & 1 & 2 & 3 & 4 \\ \hline 1 & Y_{11}^A & Y_{12}^A & 0 & 0 \\ 2 & Y_{21}^A & Y_{22}^A & 0 & 0 \\ 3 & 0 & 0 & Y_{11}^B & Y_{12}^B \\ 4 & 0 & 0 & Y_{21}^B & Y_{22}^B \end{array} \begin{array}{c|ccc} & 1' & 2' & 4' \\ \hline 1 & 1 & 0 & 0 \\ 2 & 0 & 1 & 0 \\ 3 & 1 & 0 & 0 \\ 4 & 0 & 0 & 1 \end{array}$$

$$\overleftrightarrow{Y}_{3\text{-Port}} = \begin{array}{c|ccc} & 1' & 2' & 4' \\ \hline 1' & (Y_{11}^A + Y_{11}^B) & Y_{12}^A & Y_{12}^B \\ 2' & Y_{21}^A & Y_{22}^A & 0 \\ 4' & Y_{21}^B & 0 & Y_{22}^B \end{array} \tag{5}$$

Notice that the transformation resulting from connecting ports 1 and 3 in parallel to form the new port 1' yields a Y-matrix which could have been obtained by adding rows 1 and 3 and columns 1 and 3 of $\overleftrightarrow{Y}_{SUB}$ to form the 1' row

and column of $\overleftrightarrow{Y}_{3\text{-Port}}$. Furthermore, only addition of individual subnetwork elements are required in generating $\overleftrightarrow{Y}_{3\text{-Port}}$ for the connected network.

The "new" system equation can now be written.

$$\begin{array}{|c|} \hline I'_1 \\ \hline I'_2 \\ \hline I'_4 \\ \hline \end{array} \quad \begin{array}{c} \\ 1' \\ = 2' \\ 4' \end{array} \quad \begin{array}{|c|c|c|} \multicolumn{3}{c}{\begin{array}{ccc} 1' & 2' & 4' \end{array}} \\ \hline (Y^A_{11} + Y^B_{11}) & Y^A_{12} & Y^B_{12} \\ \hline Y^A_{21} & Y^A_{22} & 0 \\ \hline Y^B_{21} & 0 & Y^B_{22} \\ \hline \end{array} \quad \begin{array}{|c|} \hline V'_1 \\ \hline V'_2 \\ \hline V'_4 \\ \hline \end{array} \tag{6}$$

This result is very promising. Is there some way other types of connections could be looked upon as parallel connections so that the same simple results can be utilized in more complex situations? To test this idea, consider the cascade connection.

2.1.2.2 Example 2

As a second example, consider the cascade connection of the two 2-ports as shown in Figure 3a. Common practice would have us multiply the individual ABCD parameters to obtain the new ABCD parameters for the cascade connection. However, we now wish to use Y-parameters, to avoid products and quotients of individual terms in our overall description, and to treat the connection as though it is "parallel" if possible. This can be accomplished as follows. Add a port 3' in parallel with port 3. Notice that the cascade connection shown in Figure 3a to form a new 2-port can now be treated as a parallel combination of ports 2 and 3 to form a new 3-port as shown in Figure 3b. If port 3' is open-circuited, then physically the networks of Figure 3a and 3b are identical. However, the mathematical descriptions are different. In the first case the resulting network is treated as a 2-port, while in the latter case it is treated as a 3-port with $I'_3 = 0$. The resulting Y-matrix for the cascade connection treated as a constrained ($I'_3 = 0$) 3-port is determined as follows. First form the Y-matrix for the unconnected subnetworks.

$$\overleftrightarrow{Y}_{SUB} = \begin{array}{c|cccc} & 1 & 2 & 3 & 4 \\ \hline 1 & Y^A_{11} & Y^A_{12} & 0 & 0 \\ 2 & Y^A_{21} & Y^A_{22} & 0 & 0 \\ 3 & 0 & 0 & Y^B_{11} & Y^B_{12} \\ 4 & 0 & 0 & Y^B_{21} & Y^B_{22} \end{array} \qquad (7)$$

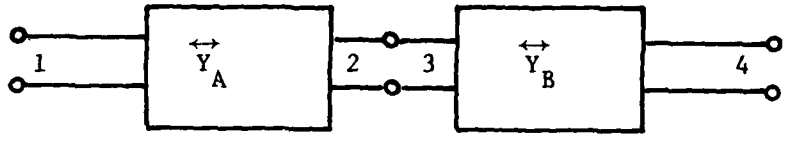

$$\overleftrightarrow{Y}_A = \begin{bmatrix} Y^A_{11} & Y^A_{12} \\ Y^A_{21} & Y^A_{22} \end{bmatrix} \qquad \overleftrightarrow{Y}_B = \begin{bmatrix} Y^B_{11} & Y^B_{12} \\ Y^B_{21} & Y^B_{22} \end{bmatrix}$$

(a)

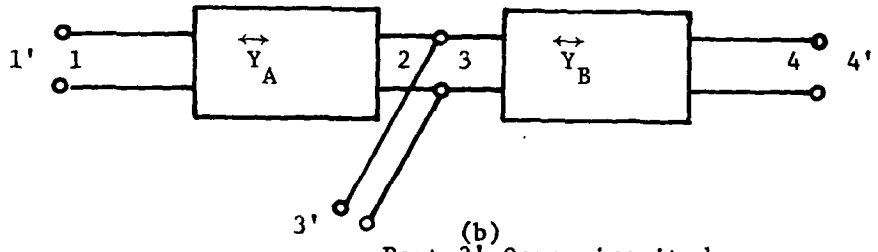

(b)
Port 3' Open-circuited

Figure 3.a) Cascade connection of 2-ports
b) Cascade connection treated as a parallel connection with added open-circuited port

The rows and columns of $\overleftrightarrow{Y}_{SUB}$ corresponding to ports to be connected in parallel are now added. Ports 2 and 3 combine to form port 3', while ports 1 and 4 become 1' and 4', respectively. The result is the desired Y-matrix for the cascade combination treated as a constrained 3-port.

$$
Y_{\substack{\text{CASCADE} \\ (I_3' = 0)}} =
\begin{array}{c|c|c|c}
 & 1' & 2' & 4' \\
\hline
1' & Y_{11}^A & Y_{12}^A & 0 \\
\hline
2' & Y_{21}^A & Y_{22}^A + Y_{11}^B & Y_{12}^B \\
\hline
4' & 0 & Y_{21}^B & Y_{22}^B
\end{array}
\tag{8}
$$

This representation of a cascade connection involves only sums of the subnetwork element admittances. The new system equation is as follows.

$$
\begin{array}{|c|}\hline I_1' \\ \hline 0 \\ \hline I_4' \\ \hline \end{array}
=
\begin{array}{c|c|c|c}
 & 1' & 2' & 4' \\
\hline
1' & Y_{11}^A & Y_{12}^A & 0 \\
\hline
2' & Y_{21}^A & Y_{22}^A + Y_{11}^B & Y_{12}^B \\
\hline
4' & 0 & Y_{21}^B & Y_{22}^B
\end{array}
\begin{array}{|c|}\hline V_1' \\ \hline V_3' \\ \hline V_4' \\ \hline \end{array}
\tag{9}
$$

The more conventional 2 by 2 matrix representation for the cascade connection can be obtained by eliminating V_3' from the system equations (recalling that $I_3' = 0$). The resulting Y-matrix is

$$
\overleftrightarrow{Y}_{\substack{\text{STANDARD} \\ \text{CASCADE}}} =
\begin{array}{c|c|c}
 & 1' & 4' \\
\hline
1' & Y_{11}^A - \dfrac{Y_{21}^A Y_{12}^A}{Y_{22}^A + Y_{11}^B} & \dfrac{-Y_{12}^B Y_{12}^A}{Y_{22}^A + Y_{11}^B} \\
\hline
4' & \dfrac{-Y_{21}^A Y_{21}^B}{Y_{22}^A + Y_{11}^B} & Y_{22}^A - \dfrac{Y_{21}^B Y_{12}^B}{Y_{22}^A + Y_{11}^B}
\end{array}
\tag{10}
$$

Which obviously includes products and quotients of individual 2-port terms, thereby considerably complicating a solution by convolution.

2.1.2.3 Example 3

True parallel connections are simple and require no added open-circuited ports. A parallel connection of one port of a 3-port network with one port of a 2-port network to form a new 4-port network is illustrated in Figure 4.

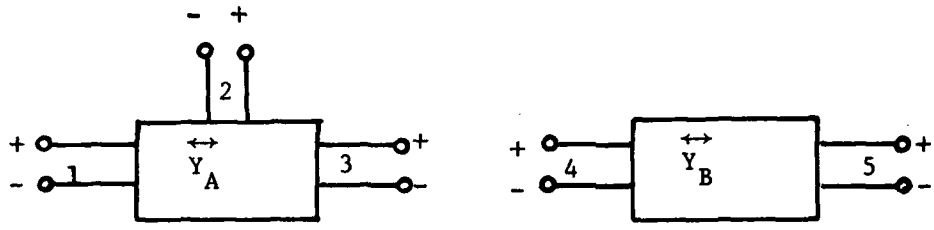

$\overleftrightarrow{Y}_{SUB}$ =

	1	2	3	4	5
1	Y^A_{11}	Y^A_{12}	Y^A_{13}	0	0
2	Y^A_{21}	Y^A_{22}	Y^A_{23}	0	0
3	Y^A_{31}	Y^A_{32}	Y^A_{33}	0	0
4	0	0	0	Y^B_{11}	Y^B_{12}
5	0	0	0	Y^B_{21}	Y^B_{22}

(a)

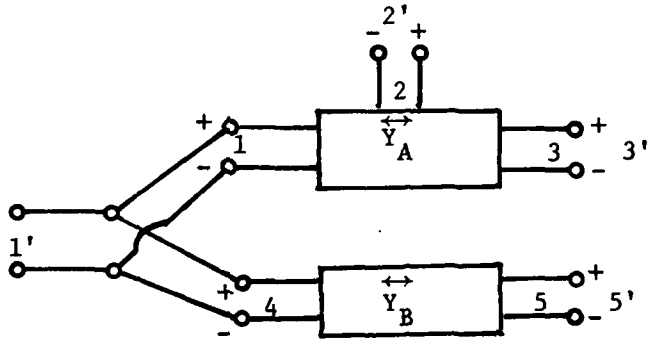

$\overleftrightarrow{Y'}$ =

	1'	2'	3'	5'
1'	$Y^A_{11}+Y^B_{11}$	Y^A_{12}	Y^A_{13}	Y^B_{12}
2'	Y^A_{21}	Y^A_{22}	Y^A_{23}	0
3'	Y^A_{31}	Y^A_{32}	Y^A_{33}	0
5'	Y^B_{21}	0	0	Y^B_{22}

(b)

Figure 4.a) Unconnected subnetworks
4.b) Ports 1 and 4 connected in parallel yielding a new 4-port network. Rows and columns 1, 4 of $\overleftrightarrow{Y}_{SUB}$ are added to $\overleftrightarrow{Y'}$

2.1.2.4 Example 4

A series interconnection of ports in terms of admittance parameters under the constraint that only sums of individual subnetwork admittance parameters appear in the result requires a little more ingenuity. An auxiliary connecting network is introduced. The series connection of a pair of ports is illustrated in Figure 5 using the networks of Figure 4a. Port 1 of network A is to be series connected to port 4 of network B. A "series T" is connected to port 1 and the Y-matrix modified as shown. This operation is easily done automatically by a computer upon receiving the command for a series connection.

2.1.2.5 Summary Comments

The series, parallel and cascade connections of pairs of ports permit very general networks to be configured from subnetworks (or elements). The very simple procedure outlined in these examples permits system equations to be formulated treating all connections as though they are parallel with the result that only sums of subnetwork admittance terms appear as desired.

2.2 SYSTEM EQUATION FORMULATION: PART 2

Returning now to the total network consisting of linear disbributed and lumped elements plus nonlinear and time-varying lumped elements. The network is partitioned as shown in Figure 1. The solution procedure is as follows. First, the short-circuit step-response matrix for the linear part of the system is established as sums of the individual subnetwork terms as described in the preceding section, then a matrix convolution equation is formed relating port voltages and currents at the interface between the linear and nonlinear network parts. The interface port voltages and currents are simultaneously constrained by the equations for the nonlinear part of the network. Both convolution and nonlinear equations are represented numerically by using trapezoidal (or another appropriate technique) integration leading to a set of simultaneous algebraic

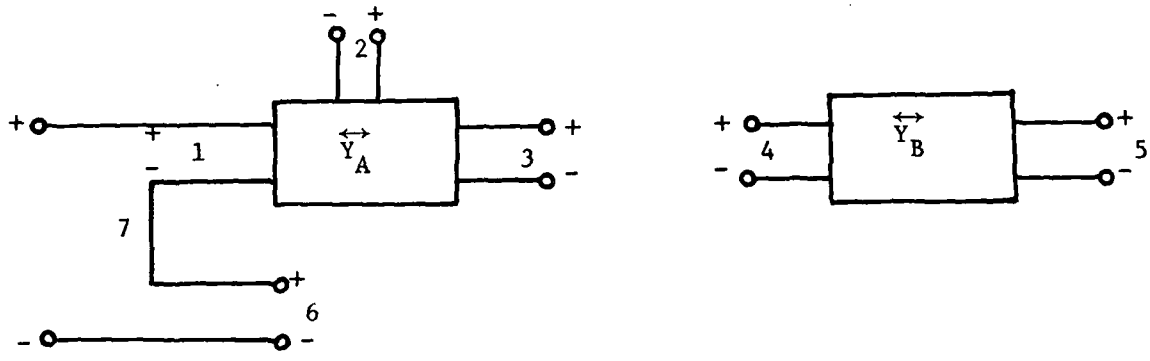

$\overleftrightarrow{Y}_{sub}$ =

	7	2	3	6	4	5
7	Y^A_{11}	Y^A_{12}	Y^A_{13}	$-Y^A_{11}$	0	0
2	Y^A_{21}	Y^A_{22}	Y^A_{23}	$-Y^A_{21}$	0	0
3	Y^A_{31}	Y^A_{32}	Y^A_{33}	$-Y^A_{31}$	0	0
6	$-Y^A_{11}$	$-Y^A_{21}$	$-Y^A_{31}$	Y^A_{11}	0	0
4	0	0	0	0	Y^B_{11}	Y^B_{12}
5	0	0	0	0	Y^B_{21}	Y^B_{22}

Figure 5a. Unconnected subnetworks with "A" modified for series connection of port 1

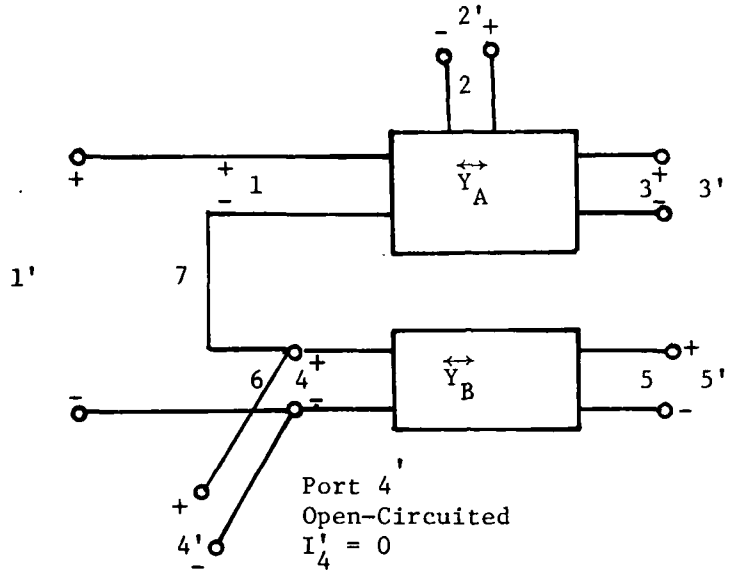

$\overleftrightarrow{Y}'$ ($I'_4 = 0$)

	1'	2'	3'	4'	5'
1'	Y^A_{11}	Y^A_{12}	Y^A_{13}	$-Y^A_{11}$	0
2'	Y^A_{21}	Y^A_{22}	Y^A_{23}	$-Y^A_{21}$	0
3'	Y^A_{31}	Y^A_{32}	Y^A_{33}	$-Y^A_{31}$	0
4'	$-Y^A_{11}$	$-Y^A_{21}$	$-Y^A_{31}$	$Y^A_{11}+Y^B_{11}$	Y^B_{12}
5'	0	0	0	Y^B_{21}	Y^B_{22}

Figure 5b. Series interconnection of port 1 of "A" with port 4 of "B"

equations relating port voltages and currents at each time increment. Solution of these equations yields desired voltages and currents at each time increment.

The step-response matrix for each linear network may be determined by measurement or calculation. Let A(s) be the step-response matrix in the Laplace-transform domain and Y(s) be the short-circuit admittance matrix. Then,

$$\overleftrightarrow{A}(s) = \frac{1}{s}\overleftrightarrow{Y}(s) \tag{11}$$

$$\overleftrightarrow{a}(t) = \mathcal{L}^{-1}\{\overleftrightarrow{A}(s)\} = \mathcal{L}^{-1}\{\frac{1}{s}\overleftrightarrow{Y}(s)\} \tag{12}$$

where $\overleftrightarrow{a}(t)$ is the step-response matrix in the time domain.

Interface port currents and voltages are constrained by the linear part of the network as follows. $\vec{I}(s)$, $\vec{V}(s)$ are vectors of port currents and voltages, respectively.

$$\vec{I}(s) = \overleftrightarrow{Y}(s)\vec{V}(s)$$

$$= \left[\frac{1}{s}\overleftrightarrow{Y}(s)\right]\left[s\ \vec{V}(s)\right] \tag{13}$$

$$\vec{i}(t) = \mathcal{L}^{-1}\{\vec{I}(s)\}\ , \text{ or}$$

$$\vec{i}(t) = \overleftrightarrow{a}(t) * \dot{\vec{v}}(t)U_{-1}(t) + \overleftrightarrow{a}(t)\vec{v}(o^{+}) \tag{14}$$

where $\dot{\vec{v}}(t)$ is the time derivative of the port voltage vector, $\vec{v}(o^{+})$ is the initial value of the port voltage vector, $U_{-1}(t)$ is a unit step, and * implies convolution. The nature of the nonlinear elements is assumed to be such that a description of the form

$$\dot{\vec{v}}(t) = \vec{f}(\vec{v}(t), \vec{i}(t), t) \tag{15}$$

is possible, where $\vec{f}(\vec{v}(t), \vec{i}(t), t)$ is a matrix whose elements are explicit functions of $\vec{v}(t)$, $\vec{i}(t)$ and t. Equations 14 and 15 describe the network completely. Given the initial conditions on $\vec{v}(t)$, we can in principle solve for $\vec{v}(t)$ and $\vec{i}(t)$ from Equations 14 and 15. Unless the matrix of functions is extremely simple, the solution must be obtained numerically. Any implicit

integration technique may be used. Trapezoidal (fixed or variable interval) and Gear type algorithms [21] have proven very satisfactory. For ease of presentation the fixed interval trapezoidal method will be presented.

Let Δ be the interval between time points. Then Equation 14 can be written as

$$\vec{i}(k\Delta) = \frac{1}{2} \sum_{j=1}^{k} \left[\overleftrightarrow{a}([k + 1 - j]\Delta) + \overleftrightarrow{a}([k - j]\Delta)\right]$$

$$x\left[\vec{v}(j\Delta) - \vec{v}([j - 1]\Delta)\right] + \overleftrightarrow{a}(k\Delta)\vec{v}(o^{+}) \qquad k = 1,2,\cdots \tag{16}$$

In each increment, the step response is approximated by the average of its two end point values and the derivative of the voltage is approximated by the divided difference of its end point values. Notice that $\vec{i}(k\Delta)$ in Equation 16 can be separated into two parts, one depending on the past history and the other on the current value of $\vec{v}(k\Delta)$, as follows:

$$\vec{i}(k\Delta) = \vec{i}_{o}(k\Delta) + \overleftrightarrow{g}_{o}\vec{v}(k\Delta) \qquad k = 1,2,\cdots \tag{17}$$

where

$$\overleftrightarrow{g}_{o} = \frac{1}{2}\left[\overleftrightarrow{a}(\Delta) + \overleftrightarrow{a}(o^{+})\right]$$

$$\vec{i}_{o}(k\Delta) = \frac{1}{2} \sum_{j=1}^{k-1} \left[\overleftrightarrow{a}([k + 1 - j]\Delta) + \overleftrightarrow{a}([k - j]\Delta)\right]\left[\vec{v}(j\Delta) - v([j - 1]\Delta)\right]$$

$$- \overleftrightarrow{g}_{o}\vec{v}([k - 1]\Delta) + \overleftrightarrow{a}(k\Delta)\vec{v}(o^{+}) \tag{18}$$

Thus, $\overleftrightarrow{g}_{o}$ is a constant matrix equal to the average step response during the first time interval. The vector $\vec{i}_{o}(k\Delta)$ can be treated as a set of current sources whose values are determined by the past history of $\vec{v}(k\Delta)$. For a given value of k, $\vec{i}_{o}(k\Delta)$ is known. In effect, a lumped, time-varying terminal equivalent circuit has been obtained for the linear (lumped-distributed) part of the overall network.

For the nonlinear part, from Equation 18 we have

$$\vec{v}(t) = \int_{t-\Delta}^{t} \vec{f}(\vec{v}(\tau), \vec{i}(\tau), \tau)d\tau + \vec{v}(t - \Delta) \ . \tag{19}$$

By the trapezoidal integration rule we have

$$\begin{aligned}\vec{v}(k\Delta) = {} & \frac{\Delta}{2} \vec{f}(\vec{v}(k\Delta) \ , \ \vec{i}(k\Delta) \ , \ k\Delta) \\ & + \frac{\Delta}{2} \vec{f}(\vec{v}([k - 1]\Delta) \ , \ \vec{i}([k - 1]\Delta) \ , \ (k - 1)\Delta) \\ & + \vec{v}([k - 1]\Delta) \qquad \text{for } k = 1,2,\cdots\end{aligned} \tag{20}$$

where $\vec{v}(k\Delta)$ is separated into two parts, one depending on the current value and the other on the past history of $\vec{v}$ and $\vec{i}$.

The solution for the overall network is obtained by solving for $\vec{v}(k\Delta)$ and $\vec{i}(k\Delta)$ simultaneously from Equations 16 and 20 at each time increment $k = 1,2,\cdots$. Note that the system of equations is algebraic even when the network contains distributed elements. The simplified flow chart of Figure 6 summarizes the solution procedure.

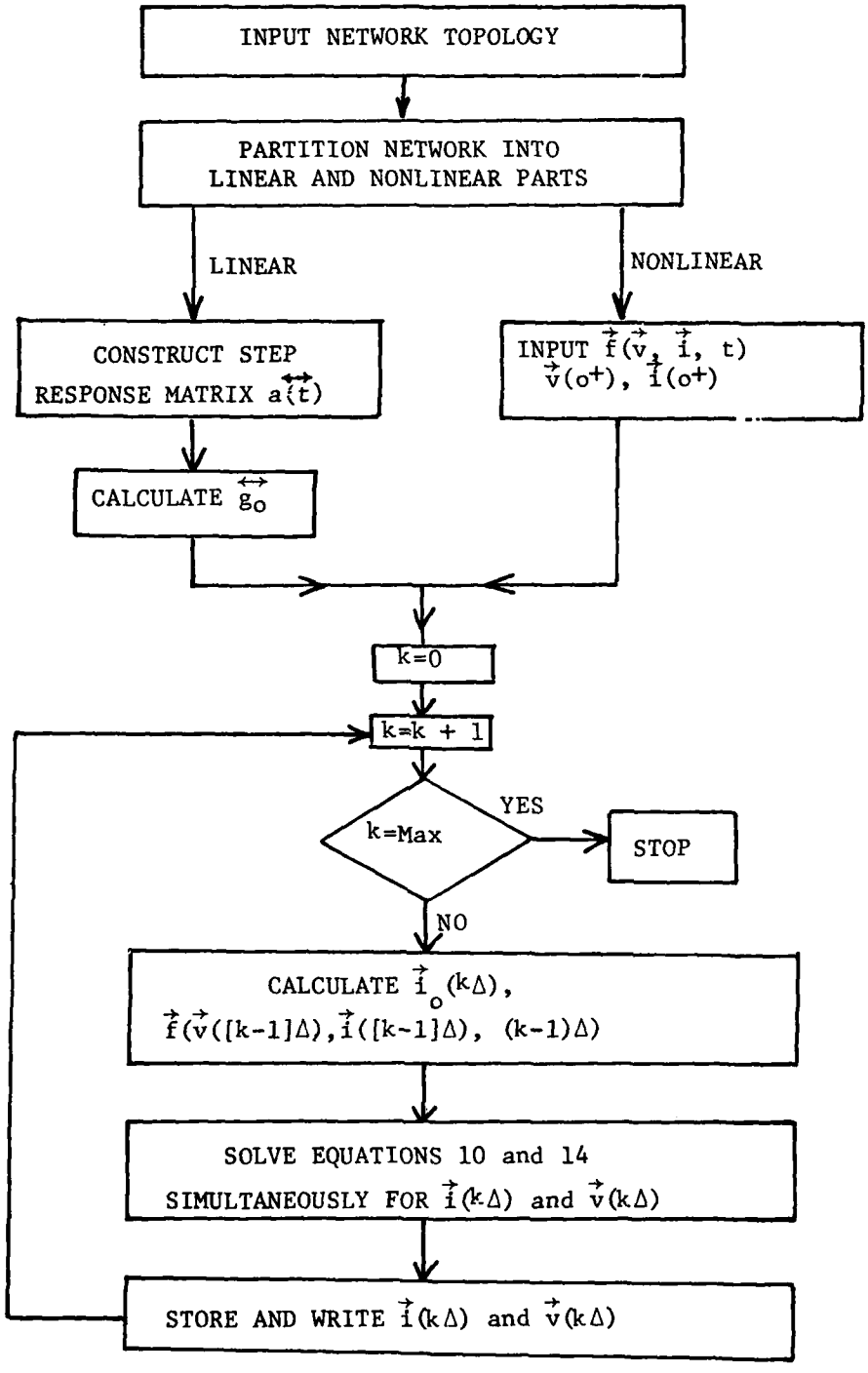

Figure 6. Simplified flow chart for solution procedure

3.0 TIME-DOMAIN EXAMPLES

The following tutorial examples were chosen such that they could be verified by hand calculations, and to clearly detail the solution procedure.

3.1 EXAMPLE 1

Three lossless transmission lines are interconnected as shown in Figure 7a. Determine the currents i_1, i_2, i_3 given that $v_g(t) = U_{-1}(t)$ volts.

The network is first redrawn, breaking the circuit into subnetworks whose step responses are known and adding open-circuited ports at any required points as shown in Figure 7b. Let $\Delta = 1$ μsec. This information is supplied to the computer causing the unconnected subnetwork matrix to be established as given in Equation 21 (zeroes are not stored).

$$\overleftrightarrow{a}_{SUB}(t) = \begin{array}{c|cccccc} & 1 & 4 & 5 & 2 & 6 & 3 \\ \hline 1 & a^A_{11} & a^A_{12} & 0 & 0 & 0 & 0 \\ 4 & a^A_{21} & a^A_{22} & 0 & 0 & 0 & 0 \\ 5 & 0 & 0 & a^B_{11} & a^B_{12} & 0 & 0 \\ 2 & 0 & 0 & a^B_{21} & a^B_{22} & 0 & 0 \\ 6 & 0 & 0 & 0 & 0 & a^C_{11} & a^C_{12} \\ 3 & 0 & 0 & 0 & 0 & a^C_{21} & a^C_{22} \end{array} \qquad (21)$$

The a_{ij}'s for these subnetworks are given in Figure 8. A variety of subnetwork terms frequently needed would be stored and available in a general purpose program. New a_{ij}'s may be input as equations, tables or measured data.

Next the interconnection information is input which, in this case, causes rows and columns 4, 5, 6 to be added yielding the connected network matrix given in Equation 22. The individual a_{ij}'s are given in Figure 8.

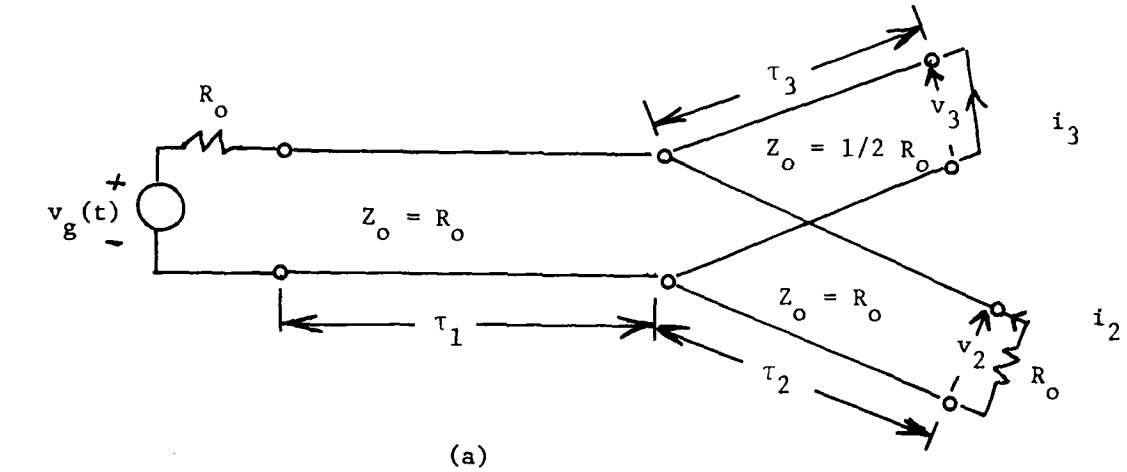

(a)

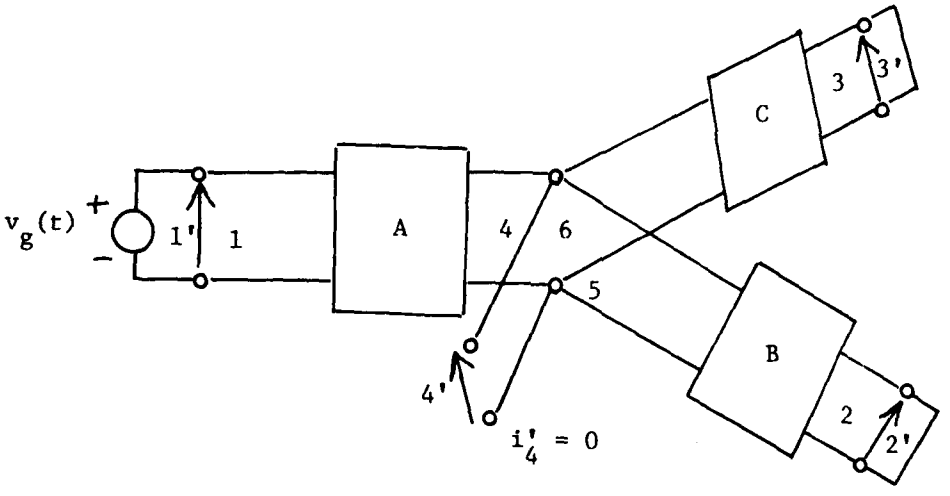

(b)

Figure 7.a) Circuit for Example 1.
$R_o = 50\ \Omega$, $\tau_1 = \tau_2 = \tau_3 = 10\ \mu$sec.
$v_g(t) = U_{-1}(t)$ volts

7.b) Block Diagram of Circuit for Example 1 Showing Added Open-Circuited Ports

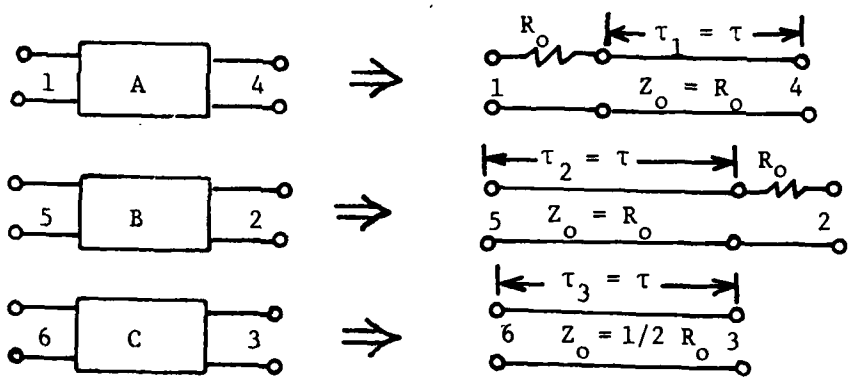

$$a_{11}^{A} = a_{22}^{B} = \frac{1}{2R_o}\left[U_{-1}(t) + U_{-1}(t - 2\tau)\right]$$

$$a_{12}^{A} = a_{21}^{A} = a_{12}^{B} = a_{21}^{B} = -\frac{1}{R_o}U_{-1}(t - \tau)$$

$$a_{22}^{A} = a_{11}^{B} = \frac{1}{R_o}U_{-1}(t)$$

$$a_{11}^{C} = a_{22}^{C} = \frac{2}{R_o}\left[U_{-1}(t) + 2U_{-1}(t - 2\tau) + 2U_{-1}(t - 4\tau) + \ldots\right]$$

$$a_{12}^{C} = a_{21}^{C} = \frac{-2}{R_o}\left[U_{-1}(t - \tau) + U_{-1}(t - 3\tau) + \ldots\right]$$

Figure 8. Subnetwork designations and step-response matrix elements

$$\overleftrightarrow{a}(t) =$$

	1	2	3	4
1	a_{11}^{A}	0	0	a_{12}^{A}
2	0	a_{22}^{B}	0	a_{21}^{B}
3	0	0	a_{22}^{C}	a_{21}^{C}
4	a_{21}^{A}	a_{12}^{B}	a_{12}^{C}	$a_{22}^{A} + a_{11}^{B} + a_{11}^{C}$

(22)

Notice that the primes have been dropped from the port designations to simplify writing the equations. Interface constraints are now imposed. In general this would involve a set of equations representing the nonlinear and source part of the system. In this example, the constraints are simply $v_1 = U_{-1}(t)$, $v_2 = 0$, $v_3 = 0$, $i_4 = 0$. Initial conditions are $v_1(o^+) = 1$, $v_2(o^+) = v_3(o^+) = v_r(o^+) = 0$.

Equation 16 can now be written for this example as

$$\begin{bmatrix} i_1(k\Delta) \\ i_2(k\Delta) \\ i_3(k\Delta) \\ 0 \end{bmatrix} = \begin{bmatrix} i_{01}(k\Delta) \\ i_{02}(k\Delta) \\ i_{03}(k\Delta) \\ i_{04}(k\Delta) \end{bmatrix} + \begin{bmatrix} \frac{1}{2R_o} & 0 & 0 & 0 & 1 \\ 0 & \frac{1}{2R_o} & 0 & 0 & 0 \\ 0 & 0 & \frac{2}{R_o} & 0 & 0 \\ 0 & 0 & 0 & \frac{4}{R_o} & v_4(k\Delta) \end{bmatrix} \tag{23}$$

where i_{01}, i_{02}, i_{03}, i_{04} must be calculated at each time increment using Equation 18.

For k = 1, $i_{01}(\Delta) = i_{02}(\Delta) = i_{03}(\Delta) = i_{04}(\Delta) = 0$, so that from Equation 23 we obtain

$$
\begin{aligned}
i_1(\Delta) &= \frac{1}{2R_o} \\
i_2(\Delta) &= 0 \\
i_3(\Delta) &= 0 \\
v_4(\Delta) &= 0
\end{aligned}
\tag{24}
$$

No change occurs in any variable until $k\Delta = \tau$. For $k = 10$, i.e., $k\Delta = \tau$, $i_{01}(10\Delta) = i_{02}(10\Delta) = 1_{03}(10\Delta) = 0$, and $i_{04}(10\Delta) = -\frac{1}{R_o}$, so that Equation 23 now yields

$$
\begin{aligned}
i_1(10\Delta) &= \frac{1}{2R_o} \\
i_2(10\Delta) &= 0 \\
i_3(10\Delta) &= 0 \\
v_4(10\Delta) &= \frac{1}{4}
\end{aligned}
\tag{25}
$$

No further change occurs until $k\Delta = 2\tau$, at which time i_1, i_2, and i_3 all change. The solution proceeds as indicated with the final results shown in Figure 9.

3.2 EXAMPLE 2

Let the network of Example 1 be modified to include a nonlinear element as shown in Figure 10. The input voltage is now $v_g(t) = t\, U_{-1}(t)$ for $t \leq 2$ μsec and $v_g(t) = 0$ for $t > 2$ μsec. All other parameters for Example 1 remain unchanged. Determine $v_2(t)$ and $v_3(t)$.

The setup for Example 1 remains unchanged except for the new input voltage and the constraint imposed on the output port of block "C" by the nonlinear device. With $\Delta = 0.5$ μsec and the proper nonlinear constraint imposed, the program yields the results of Figure 11, which can be easily verified by hand calculations.

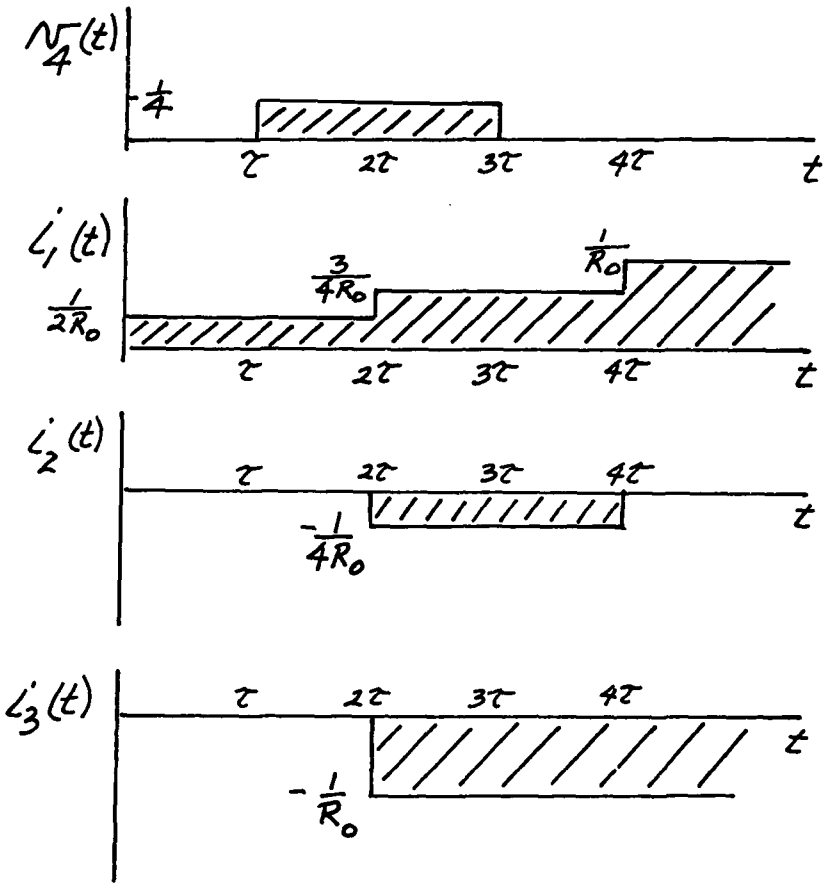

Figure 9. Solution for Example 1, volts, amps.

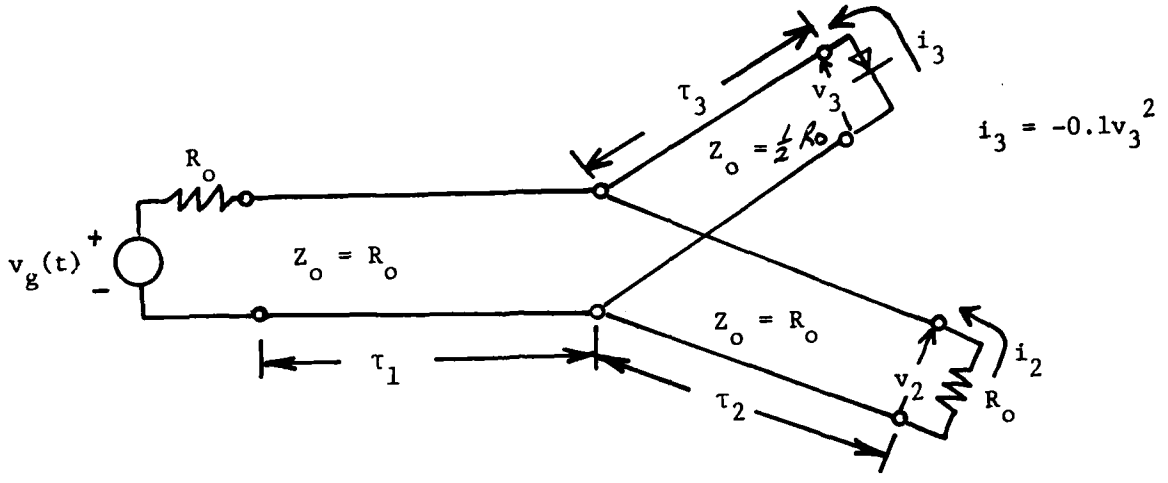

Figure 10. Circuit for Example 2.

$R_o = 500\ \Omega$, $\tau_1 = \tau_2 = \tau_3 = 10\ \mu sec$

$v_g(t) = tU_{-1}(t)$ for $t \leq 2\ \mu sec$

$= 0$ for $t > 2\ \mu sec$

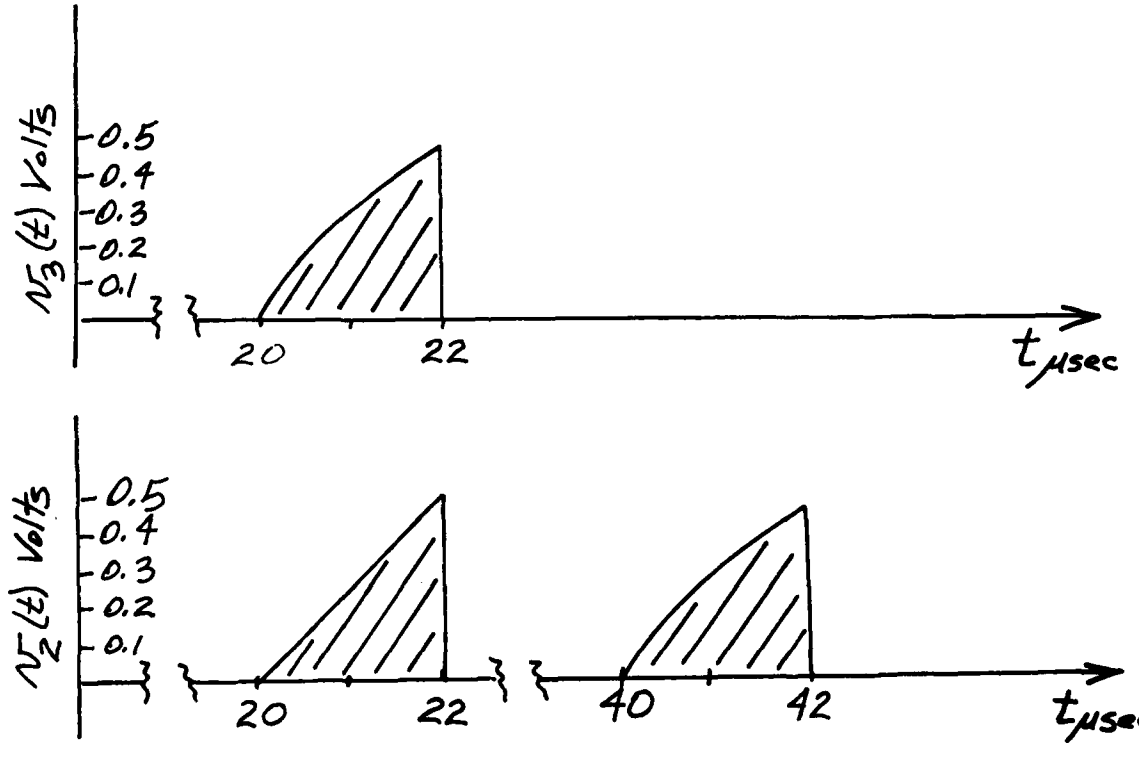

Figure 11. Solution for Example 2, volts.

3.3 EXAMPLE 3

A network consisting of three sections of lossy but distortionless transmission lines with RC loads as shown in Figure 12 is driven by a step current generator. Determine $v_1(t)$ and $v_2(t)$. This example is one used by Silverberg [4]. The exact solutions for this problem are

$$\begin{aligned} v_1(t) &= (1 - e^{-t}) \text{ volts} \\ v_2(t) &= (e^{-0.5} - e^{-t})U_{-1}(t - 0.5) \text{ volts} . \end{aligned} \tag{26}$$

Results computed by the computer program are shown in Figure 13 and agree with the exact results to six decimal places.

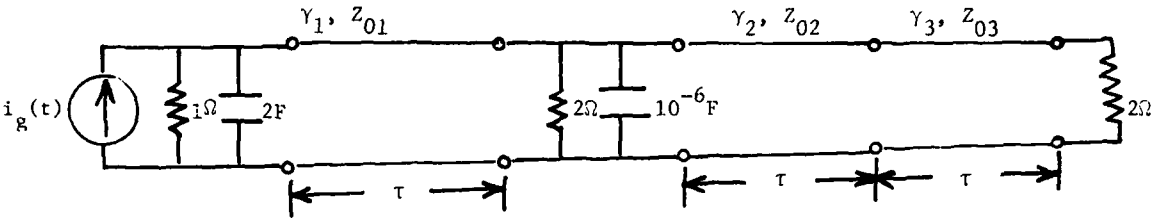

Figure 12. Circuit for Example 3.

$i_g(t) = 2U_{-1}(t)$ Amps

$\tau = 0.5$ sec, $\gamma_1 = \gamma_2 = \gamma_3 = s + 1$

$Z_{01} = 1\ \Omega$, $Z_{02} = Z_{03} = 2\ \Omega$

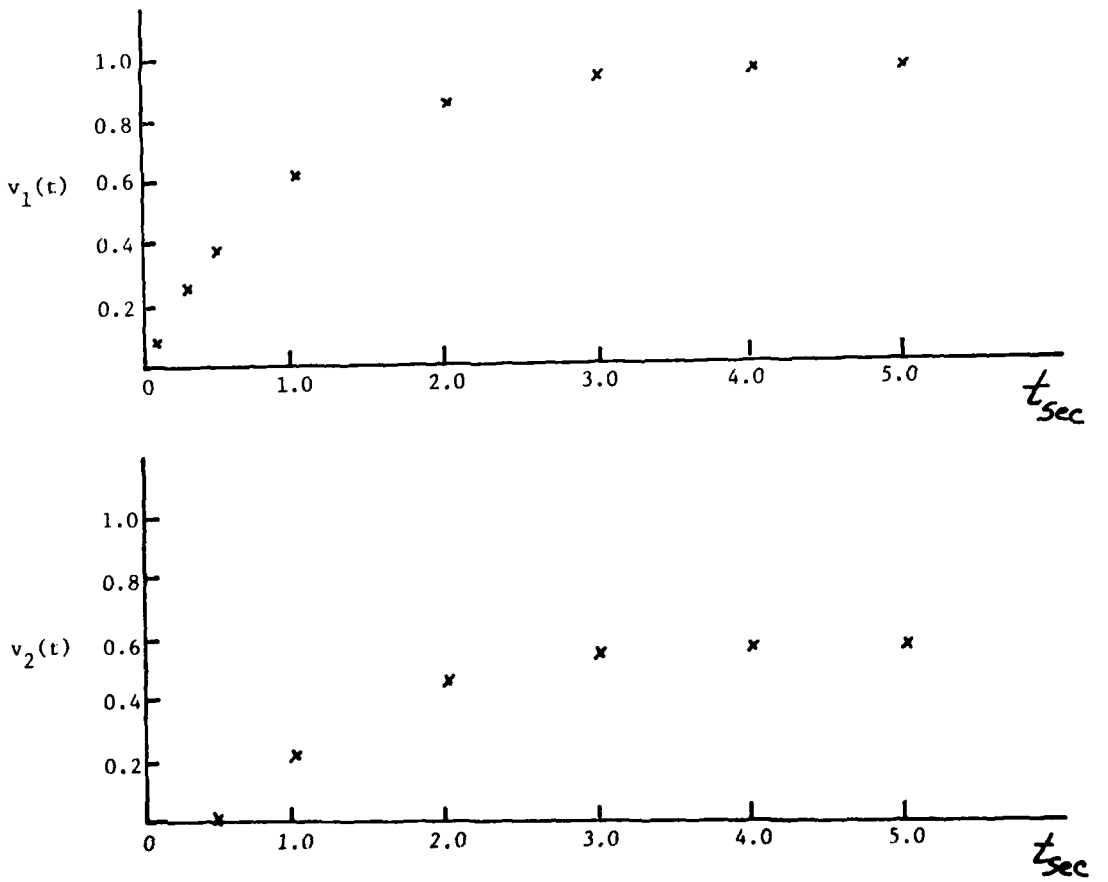

Figure 13. Solution for Example 3, volts.

4.0 FREQUENCY-DOMAIN EXAMPLE

As pointed out in Section 1.0, the same procedure can be used to formulate either time-domain or frequency-domain system equations which utilize only sums or differences of individual subnetwork matrix elements. The resulting system matrix is in both cases usually quite sparse with the associated computational efficiency. The general procedure for the frequency domain is illustrated by the following example.

Given the network consisting of transmission lines connected to a lumped element junction as shown in Figure 14, determine the average power dissipated in the 40 ohm, 60 ohm and 50 ohm resistors. Redraw the network adding open-circuited ports as needed (note that this step is not unique and a number of usable combinations can be generated). The result is shown in Figure 15.

It is sometimes convenient (particularly if the analysis program can be used on an interactive basis) to create the final system matrix as a sequence of steps involving only two of the subnetworks at a time. This procedure is illustrated with the current example as follows.

Given

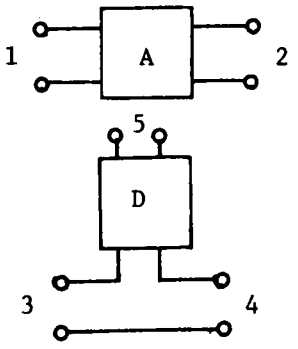

	1	2
1	Y^A_{11}	Y^A_{12}
2	Y^A_{21}	Y^A_{22}

	3	4	5
3	Y^D_{11}	$-Y^D_{11}$	Y^D_{12}
4	$-Y^D_{11}$	Y^D_{11}	$-Y^D_{12}$
5	Y^D_{21}	$-Y^D_{21}$	Y^D_{22}

to be combined as follows.

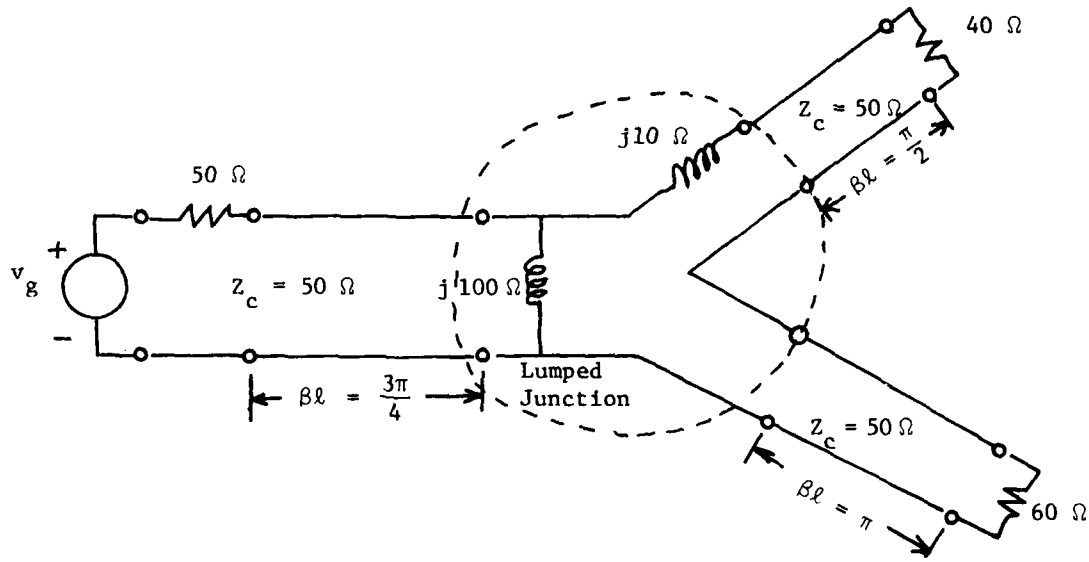

Figure 14. Circuit for frequency-domain example. V_g = 10 volts peak.

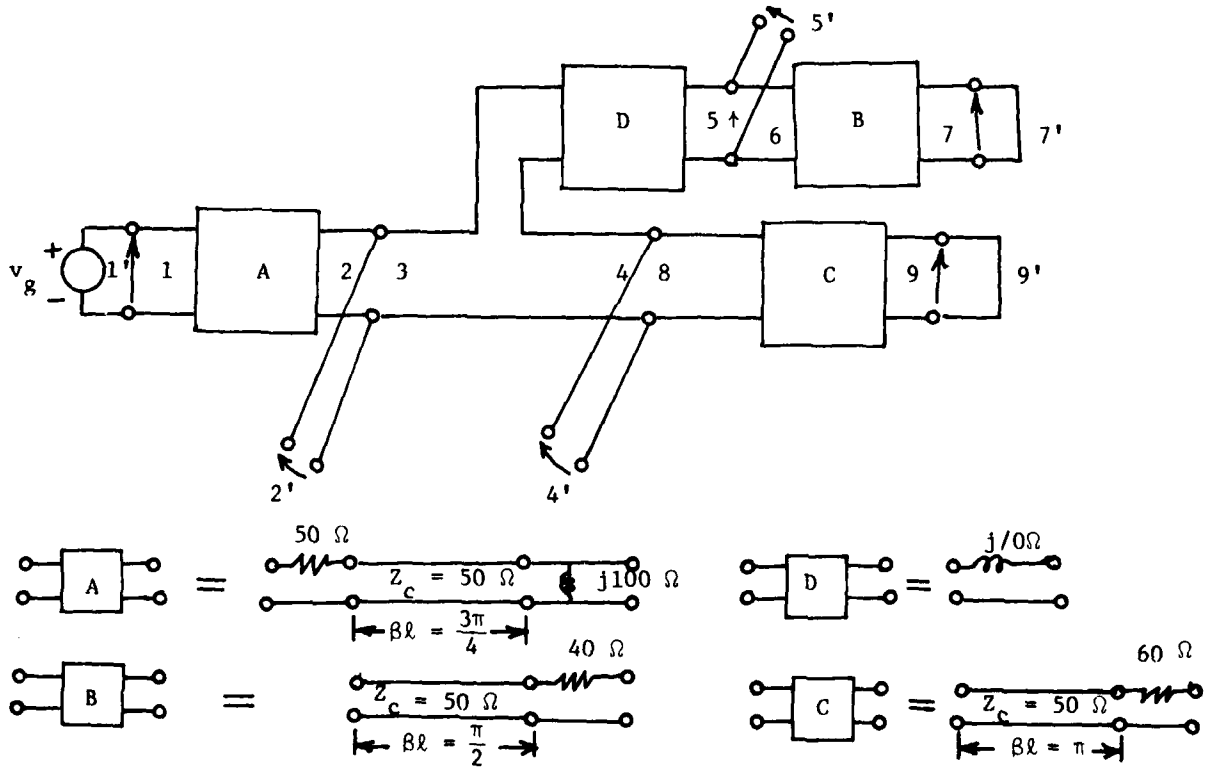

Figure 15. Block diagram with added open-circuited ports for circuit of Figure 14.

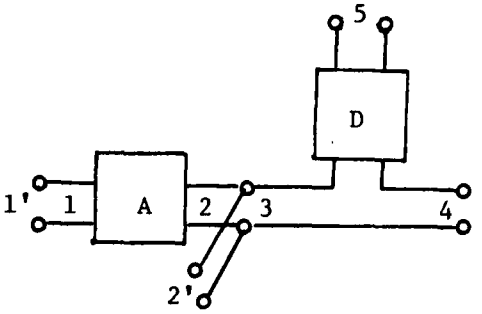

Form the matrix for the unconnected subnetworks.

$$\overleftrightarrow{Y}_{SUB\ 1} = \begin{array}{c|ccccc} & 1 & 2 & 3 & 4 & 5 \\ \hline 1 & Y^A_{11} & Y^A_{12} & 0 & 0 & 0 \\ 2 & Y^A_{21} & Y^A_{22} & 0 & 0 & 0 \\ 3 & 0 & 0 & Y^D_{11} & -Y^D_{11} & Y^D_{12} \\ 4 & 0 & 0 & -Y^D_{11} & Y^D_{11} & -Y^D_{12} \\ 5 & 0 & 0 & Y^D_{21} & -Y^D_{21} & Y^D_{22} \end{array} \qquad (27)$$

Add columns and rows 2 and 3 to obtain the new matrix representing the interconnection to this point.

$$\overleftrightarrow{Y}_{Intermediate\ 1} = \begin{array}{c|cccc} & 1' & 2' & 4 & 5 \\ \hline 1' & Y^A_{11} & Y^A_{12} & 0 & 0 \\ 2' & Y^A_{21} & Y^A_{22} + Y^D_{11} & -Y^D_{11} & Y^D_{12} \\ 4 & 0 & -Y^D_{11} & Y^D_{11} & -Y^D_{12} \\ 5 & 0 & Y^D_{21} & -Y^D_{21} & Y^D_{22} \end{array} \qquad (28)$$

Continuing with the next step,

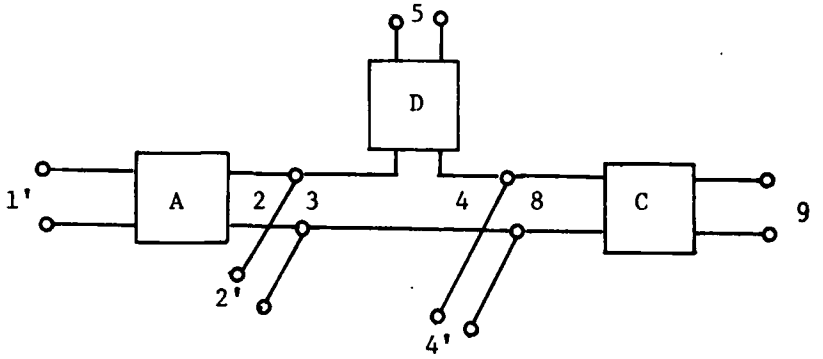

$$\overleftrightarrow{Y}_{SUB\ 2} =$$

	1'	2'	4	5	8	9'
1'	Y_{11}^{A}	Y_{12}^{A}	0	0	0	0
2'	Y_{21}^{A}	$Y_{22}^{A} + Y_{11}^{D}$	$-Y_{11}^{D}$	Y_{12}^{D}	0	0
4	0	$-Y_{11}^{D}$	Y_{11}^{D}	$-Y_{12}^{D}$	0	0
5	0	Y_{21}^{D}	$-Y_{21}^{D}$	Y_{22}^{D}	0	0
8	0	0	0	0	Y_{11}^{C}	Y_{12}^{C}
9'	0	0	0	0	Y_{21}^{C}	Y_{22}^{C}

(29)

Add rows and columns 4 and 8 to obtain the new matrix representing the interconnection with "C" added.

$$\overleftrightarrow{Y}_{Intermediate\ 2} =$$

	1'	2'	4'	5	9'
1'	Y_{11}^{A}	Y_{12}^{A}	0	0	0
2'	Y_{21}^{A}	$Y_{22}^{A} + Y_{11}^{D}$	$-Y_{11}^{D}$	Y_{12}^{D}	0
4'	0	$-Y_{11}^{D}$	$Y_{11}^{D} + Y_{11}^{C}$	$-Y_{21}^{D}$	Y_{12}^{C}
5	0	Y_{21}^{D}	$-Y_{21}^{D}$	Y_{22}^{D}	0
9'	0	0	Y_{21}^{C}	0	Y_{22}^{C}

(30)

The next step is to connect subnetwork "B."

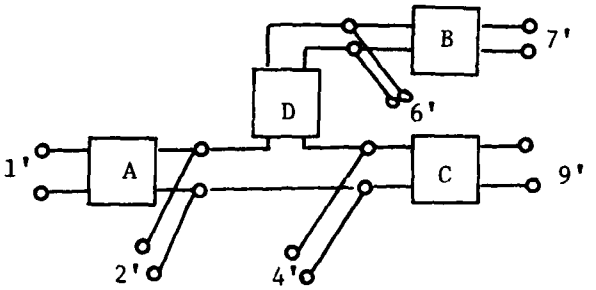

$$\overleftrightarrow{Y}_{SUB\ 3} = \begin{array}{|c|cc|l} \hline \overleftrightarrow{Y}_{Intermediate\ 2} & \overleftrightarrow{0} & & \\ \hline \multirow{2}{*}{$\overleftrightarrow{0}$} & Y^B_{11} & Y^B_{12} & 6 \\ & Y^B_{21} & Y^B_{22} & 7' \\ \hline & 6 & 7' & \end{array} \qquad (31)$$

Add rows and columns 5 and 6 to obtain the new matrix representing the final step of interconnection in which network "B" is connected. The result for the entire combined network is as follows.

$$\overleftrightarrow{Y}_{new} = \begin{array}{c|cccccc} & 1' & 2' & 4' & 5' & 7' & 9' \\ \hline 1' & Y^A_{11} & Y^A_{12} & 0 & 0 & 0 & 0 \\ 2' & Y^A_{21} & Y^A_{22} + Y^D_{11} & -Y^D_{11} & Y^D_{12} & 0 & 0 \\ 4' & 0 & -Y^D_{11} & Y^D_{11} + Y^C_{11} & -Y^D_{12} & 0 & Y^C_{12} \\ 5' & 0 & Y^D_{21} & -Y^D_{21} & Y^B_{11} + Y^D_{22} & Y^B_{12} & 0 \\ 7' & 0 & 0 & 0 & Y^B_{21} & Y^B_{22} & 0 \\ 9' & 0 & 0 & Y^C_{21} & 0 & 0 & Y^C_{22} \end{array} \qquad (32)$$

From Figure 15 the output ports 7' and 9' are short circuited and ports 2', 4' and 5' are open circuited, so that

$$v_7' = v_9' = 0 \quad \text{and} \quad i_2' = i_4' = i_5' = 0 \ .$$

The input is given as $v_1' = 10$ volts peak. The system equation for the combined network is thus

$$\begin{bmatrix} i_1' \\ 0 \\ 0 \\ 0 \\ i_7' \\ i_9' \end{bmatrix} = \overleftrightarrow{Y}_{new} \begin{bmatrix} 10 \\ v_2' \\ v_4' \\ v_5' \\ 0 \\ 0 \end{bmatrix} \tag{33}$$

These equations can be straightforwardly solved for the currents i_1', i_7', and i_9' and the voltages v_2', v_4', v_5' since all elements of $\overleftrightarrow{Y}_{new}$ are known. From these currents calculate the power delivered to the resistors. The 40 Ω resistor receives 91.6 mwatts, the 60 Ω resistor 87.9 mwatts, and the 50 Ω resistor 70.5 mwatts.

5.0 TIME-DOMAIN MODELS FOR TRANSMISSION LINES

The techniques of Section 2.2 provide not only a very general analysis tool, but also provide a powerful scheme for generating simple time-domain models for complex structures. Modeling will be illustrated for lossless transmission lines. Lossy transmission lines, coupled lines and other structures will be covered in a future report. These models may be used to increase the power of existing general purpose circuit analysis programs such as SCEPTRE or SPICE by providing transmission line and other distributed element capability not currenlty available. Alternatively, the models may form the basis of new analysis programs.

5.1 STEP-RESPONSE OF LOSSLESS TRANSMISSION LINES

A necessary ingredient for time-domain model derivation using the techniques of Section 2.2 is the short-circuit current step response of the structure to be modeled. This step response may be determined experimentally or analytically. For the lossless transmission line the step response may be determined as follows.

5.1.1 Unterminated Line

Figure 16 shows schematically a lossless transmission line of length, "ℓ," characteristic admittance "G_o," and propagation factor '$j\beta$." Since $j\beta = j\omega\ell/v$, where ω is radian frequency and v is phase velocity, $j\beta\ell$ corresponds to $j\beta\tau$, where τ is ℓ/v equal to the one-way time delay through the line. Next, transform to the Laplace transform domain replacing $j\omega$ by s (the Laplace variable).

The admittance matrix for the lossless transmission line in the Laplace domain is

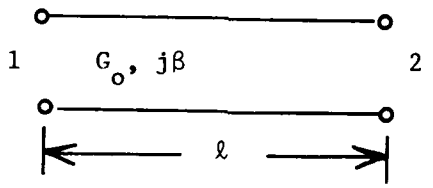

$$j\beta\ell = j\omega\ \ell/v = j\omega\tau \leftrightarrow s\tau$$

Figure 16. Lossless, Unterminated Transmission Line

$$\overleftrightarrow{Y}(s) = G_o \begin{array}{|c|c|} \hline \coth s\tau & \dfrac{-1}{\sinh s\tau} \\ \hline \dfrac{-1}{\sinh s\tau} & \coth s \\ \hline \end{array} \tag{34}$$

which can be written in terms of exponentials as follows.

$$\overleftrightarrow{Y}(s) = G_o \begin{array}{|c|c|} \hline \dfrac{e^{s\tau} + e^{-s\tau}}{e^{s\tau} - e^{-s\tau}} & \dfrac{-2}{e^{s\tau} - e^{-s\tau}} \\ \hline \dfrac{-2}{e^{s\tau} - e^{-s\tau}} & \dfrac{e^{s\tau} + e^{-s\tau}}{e^{s\tau} - e^{-s\tau}} \\ \hline \end{array} \tag{35}$$

Dividing the denominator of each term into the numerator yields the following form.

$$\overleftrightarrow{Y}(s) = G_o \begin{array}{|c|c|} \hline Y_{11} & Y_{12} \\ \hline Y_{21} & Y_{22} \\ \hline \end{array} \tag{36}$$

where

$$Y_{11} = Y_{22} = 1 + 2\ \{e^{-2s\tau} + e^{-4s\tau} + \cdots\}$$

$$Y_{12} = Y_{21} = -2\ \{e^{-s\tau} + e^{-3s\tau} + e^{-5s\tau} + \cdots\}$$

Taking the inverse Laplace transform of Y(s) would yield the time-domain impulse response. The step response is obtained from the inverse transform of $\frac{1}{s}\overleftrightarrow{Y}(s)$. Designate the step-response matrix by $\overleftrightarrow{a}(t)$.

$$\overleftrightarrow{a}(t) = \mathcal{L}^{-1}\ \frac{1}{s}\,Y(s) \quad = \begin{array}{|c|c|} \hline a_{11}(t) & a_{12}(t) \\ \hline a_{21}(t) & a_{22}(t) \\ \hline \end{array} \tag{37}$$

where

$$a_{11} = a_{22} = G_o\{U_{-1}(t) + 2U_{-1}(t - 2\tau) + 2U_{-1}(t - 4\tau) + \cdots\}$$

$$a_{12} = a_{21} = -2G_o\{U_{-1}(t - \tau) + U_{-1}(t - 3\tau) + U_{-1}(t - 5\tau) + \cdots\}$$

and $U_{-1}(\cdot)$ is the unit step function.

5.1.2 "Properly" Terminated Lines

If a "proper" G_o termination is used on the input or output of the lossless transmission line, the step response reduces to a simple closed form rather than the infinite series of the unterminated line. The properly terminated form has some advantages when used with SCEPTRE and SPICE. If a termination different from G_o is desired, an appropriate negative or positive resistor is inserted in series with the G_o termination. Figure 17 gives the step response for input and output terminated lines.

5.2 ASSOCIATED MODEL

Each model is associated with (or derived using) a particular numerical integration algorithm. Trapezoidal integration will be used in the illustrations.

Consider the input terminated line of Figure 17a. From Section 2.2 (Eq. 14)

$$\vec{i}(t) = \overleftrightarrow{a}(t) * \dot{\vec{v}}(t) + \overleftrightarrow{a}(t)\vec{v}(0^+) \tag{38}$$

For fixed time increment "Δ," the discretized form of Equation 38 is

$$\vec{i}(k\Delta) = \vec{i}_o(k\Delta) + \overleftrightarrow{g}_o\vec{v}(k\Delta) \tag{39}$$

where $\vec{i}_o(k\Delta)$ is a function of past values only and $\overleftrightarrow{g}_o$ is a constant. This means that only $\vec{i}(k\Delta)$ and $\vec{v}(k\Delta)$ are functions of the current time increment, $k\Delta$. The discretized equation for the transmission line of Figure 17a takes the following form.

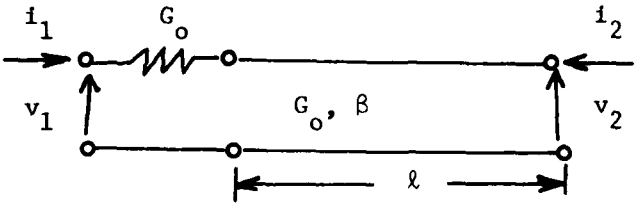

$$\overleftrightarrow{a}(t) = \begin{array}{|c|c|}\hline a_{11} & a_{12} \\ \hline a_{21} & a_{22} \\ \hline \end{array}$$

where $a_{11} = \frac{G_o}{2}\,[U_{-1}(t) + U_{-1}(t - 2\tau)]$

$a_{12} = a_{21} = -G_o U_{-1}(t - \tau)$

$a_{22} = G_o U_{-1}(t)$

(a)

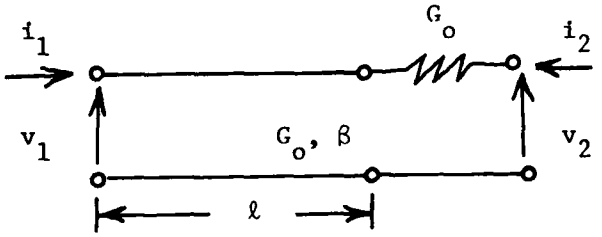

$$\overleftrightarrow{a}(t) = \begin{array}{|c|c|}\hline a_{11} & a_{12} \\ \hline a_{21} & a_{22} \\ \hline \end{array}$$

where $a_{11} = G_o U_{-1}(t)$

$a_{12} = a_{21} = -G_o U_{-1}(t - \tau)$

$a_{22} = \frac{G_o}{2}\,[U_{-1}(t) + U_{-1}(t - 2\tau)]$

(b)

Figure 17.a) Step Response for Input Terminated Line
b) Step Response for Output Terminated Line

$$\begin{bmatrix} i_1(k\Delta) \\ i_2(k\Delta) \end{bmatrix} = \begin{bmatrix} i_{01}(k\Delta) \\ i_{02}(k\Delta) \end{bmatrix} + \begin{bmatrix} g_{11} & g_{12} \\ g_{21} & g_{22} \end{bmatrix} \begin{bmatrix} v_1(k\Delta) \\ v_2(k\Delta) \end{bmatrix} \tag{40}$$

where

$$g_{11} = \frac{1}{2}\left[a_{11}(\Delta) + a_{11}(0^+)\right] = \frac{G_o}{2}$$

$$g_{12} = \frac{1}{2}\left[a_{12}(\Delta) + a_{12}(0^+)\right] = 0$$

$$g_{21} = \frac{1}{2}\left[a_{21}(\Delta) + a_{21}(0^+)\right] = 0$$

$$g_{22} = \frac{1}{2}\left[a_{22}(\Delta) + a_{22}(0^+)\right] = G_o$$

Thus, $i_{01}(k\Delta)$ and $i_{02}(k\Delta)$ may be interpreted as dependent current sources whose values may be calculated from results obtained at prior time increments. The simple model of Figure 18 results.

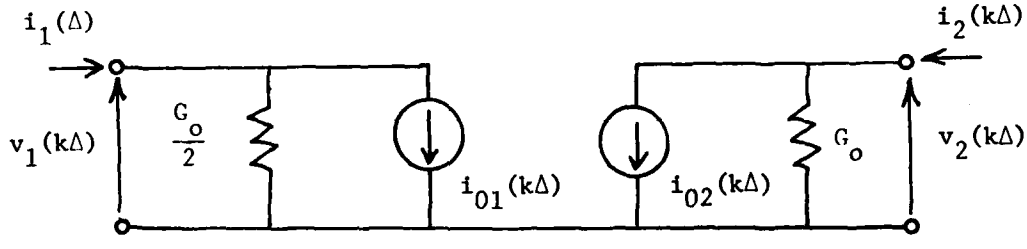

Figure 18. Lossless Transmission Line Model

The two dependent current sources can be evaluated from Equation 39. For $k = 0$, $v_1(0)$ and $v_2(0)$ must be supplied as initial conditions. For $k \geq 1$

$$i_{01}(k\Delta) = \frac{G_o v_1(0)}{2}[1 + U_{-1}(k\Delta - 2\tau)] - v_2(0)G_o U_{-1}(k\Delta - \tau)$$

$$- \frac{G_o}{2} v_1((k-1)\Delta) + \frac{G_o}{4} \sum_{j=1}^{k-1} \{[2 + U_{-1}((k-j+1)\Delta - 2\tau)$$

$$+ U_{-1}((k-j)\Delta - 2\tau)][v_1(j\Delta) - v_1((j-1)\Delta)]$$

$$- 2[U_{-1}((k-j+1)\Delta - \tau) + U_{-1}((k-j)\Delta - \tau)][v_2(j\Delta) - v_2((j-1)\Delta)]\} \quad (41)$$

$$i_{02}(k\Delta) = -G_o v_1(0)U_{-1}(k\Delta - \tau) + G_o v_2(0) - G_o v_2((k-1)\Delta)$$

$$+ \frac{G_o}{2} \sum_{j=1}^{k-1} \{2[v_2(j\Delta) - v_2((j-1)\Delta)] - [U_{-1}((k-j+1)\Delta - \tau)$$

$$+ U_{-1}((k-j)\Delta - \tau)][v_1(j\Delta) - v_1((j-1)\Delta)]\} \quad (42)$$

These equations are easily implemented yielding an efficient transmission line model for time-domain calculations.

6.0 INSTANTANEOUS REFELCTION COEFFICIENT

A very general concept that appears quite promising in dealing with complex circuits is that of a time-varying reflection coefficient. When used in conjunction with "fractional time" techniques, the time-varying reflection coefficient permits certain types of energy relationships to be deduced in a simple fashion. To demonstrate the principle, consider the circuit shown in Figure 19. The circuit consists of a lossless transmission line driven by a triangular voltage pulse. Generator impedance is identical to the characteristic impedance of the transmission line. Terminating the line is a nonlinear resistor whose characteristics (see Figure 19b) are such that for terminal voltage amplitudes less than V_1 the resistor looks like an open circuit. For voltages between V_1 and V_2, the resistor has a resistance of Z_o ohms, i.e., equal to the transmission line characteristic impedance. For voltages greater than V_2 the terminating resistor looks like a short circuit. Thus, the reflection coefficient, ρ, of this resistor as viewed from the transmission line will be a function of the terminal voltage and, since that voltage is time-varying, the reflection coefficient is itself time varying. In fact, the reflection coefficient is $\rho = +1$ for voltages less than V_1, $\rho = 0$ for voltages between V_1 and V_2, and $\rho = -1$ for voltages greater than V_2. The fraction of incident instantaneous power absorbed by the nonlinear resistor is $1 - \rho^2$. The voltage interval $V_1 \rightarrow V_2$ during which power is absorbed and the corresponding time intervals for a triangular input pulse are shown in Figures 19c and 19d. As can be seen from the sketches, the fractional time for which $\rho = 0$ decreases as the input pulse amplitude increases. Since in this case power is absorbed only when $\rho = 0$, the total energy (product of time and power) absorbed by the nonlinear resistor decreases as the input pulse amplitude increases. The energy reflected by the nonlinear termination is absorbed by

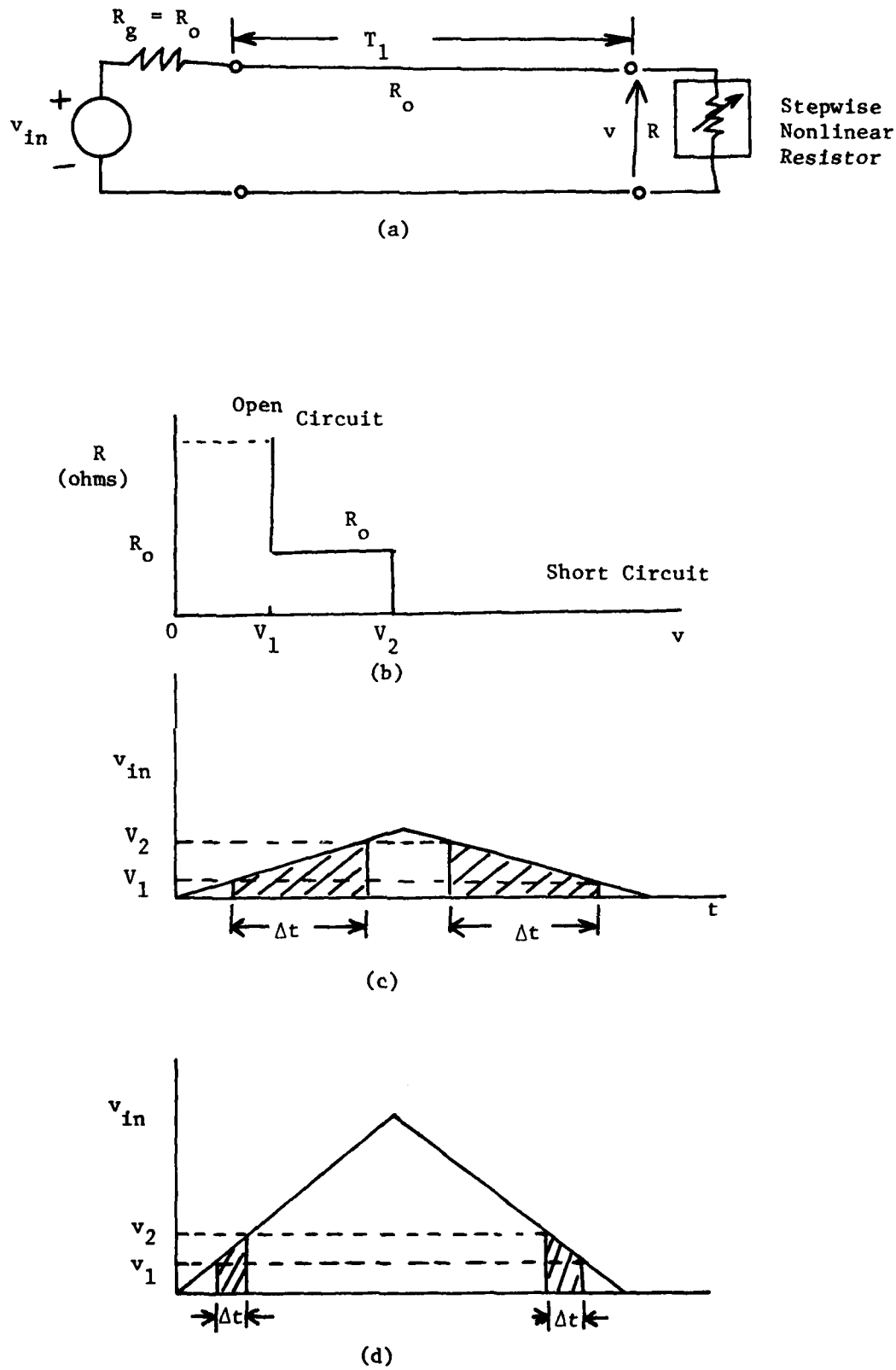

Figure 19. Instantaneous Reflection Coefficient and Fractional Time Calculations for Predicting Bounds on Absorbed Energy (Explanation in text)

the matched load at the source end of the line. The interesting point is that for this and related type v - i characteristic nonlinear devices, one can say that if the input energy increases by a factor K, the energy absorbed by the device will increase by a factor less than K, i.e, linear extrapolation provides an upper bound estimate for energy absorbed.

Many semiconductor elements have v - i characteristics that yield results similar to that of the above example. As another simple example, consider a square-law diode on the end of a transmission line, as shown in Figure 20a. Since the v - i relation for the diode is

$$i_d = kV_d^2 \tag{43}$$

where k is a constant, the instantaneous admittance of the diode is

$$y_d = \frac{i_d}{v_d} = kv_d \ . \tag{44}$$

Diode reflection coefficient referenced to the transmission line is

$$\rho_d = \frac{Y_o - kV_d}{Y_o + kV_d} \tag{45}$$

and after some algebra

$$1 - \rho_d^2 = \frac{4kY_o V_d}{(kV_d + Y_o)^2} \tag{46}$$

A plot of $1 - \rho_d^2$ versus V_d is given in Figure 20b. The percentage of incident power absorbed by the diode first increases and then decreases with increasing terminal voltage. Maximum absorbed power occurs at the "match point" where the apparent resistance of the diode is equal to the characteristic impedance of the transmission line.

Interpretation of power absorbed in terms of time-varying instantaneous reflection coefficient also applies to circuits with reactance. To illustrate this point of view a sequence of parallel connected ideal lumped elements are

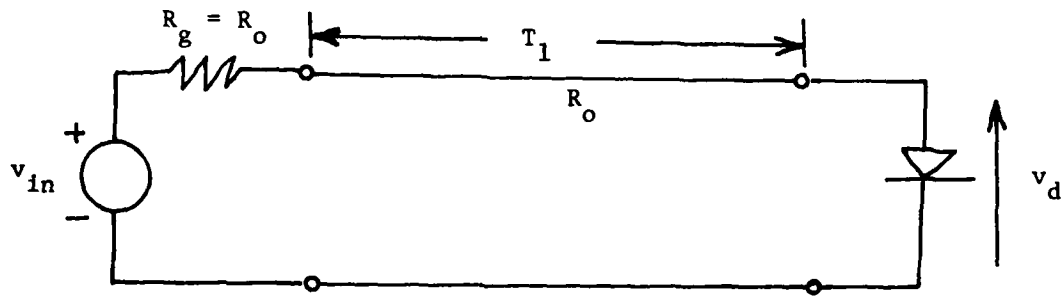

(a)

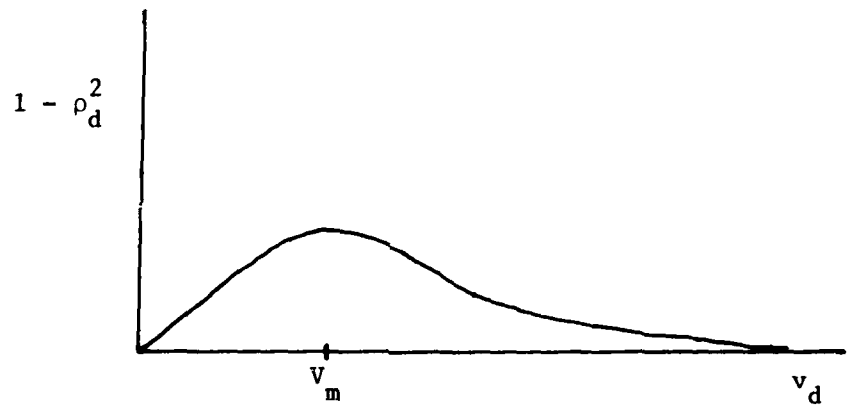

(b)

Figure 20. Percent Power Absorbed by Diode as a Function of Diode Voltage

considered as depicted in Figure 21. Each of the circuits is considered to be driven by a sinusoidal current source in parallel with a resistance. This source could represent a Norton equivalent of a transmission line.

In Figure 21a a single resistor is driven by the source. The instantaneous impedance of the load resistor is independent of time and its reflection coefficient is a real constant. Instantaneous power absorbed is

$$P_R = V_R i_R = \frac{I_o^2 R_p^2}{R} \sin^2 \omega t \tag{47}$$

where

$$R_p = \frac{RR_o}{R + R_o} .$$

Time average power absorbed is

$$P_{avg} = R_p^2 \, I_o^2 / 2R \tag{48}$$

Now consider what happens when a shunt capacitor is introduced as shown in Figure 21b.

The capacitor alone has an instantaneous impedance given by

$$Z_C(t) = \frac{V_C}{C\dot{V}_C} = \frac{\frac{1}{C}\int i_C dt}{i_C} = \frac{V_C}{i_C} \tag{49}$$

where $\dot{V}_C$ = time derivative of $V_C(t)$. For a sinusoidal input the instantaneous impedance of the capacitor varies from zero (or short circuit) to infinite (or open circuit) each quarter cycle and is given by

$$Z_C(t)\Big|_{\sin} = \frac{1}{\omega C} \tan \omega t \tag{50}$$

Thus, in Figure 21b the constant instantaneous impedance of the resistor R is now paralleled by a time-varying instantaneous resistance that varies from a short circuit to an open circuit each quarter cycle. Since the time-varying reflection coefficient of the parallel RC combination will now deviate from

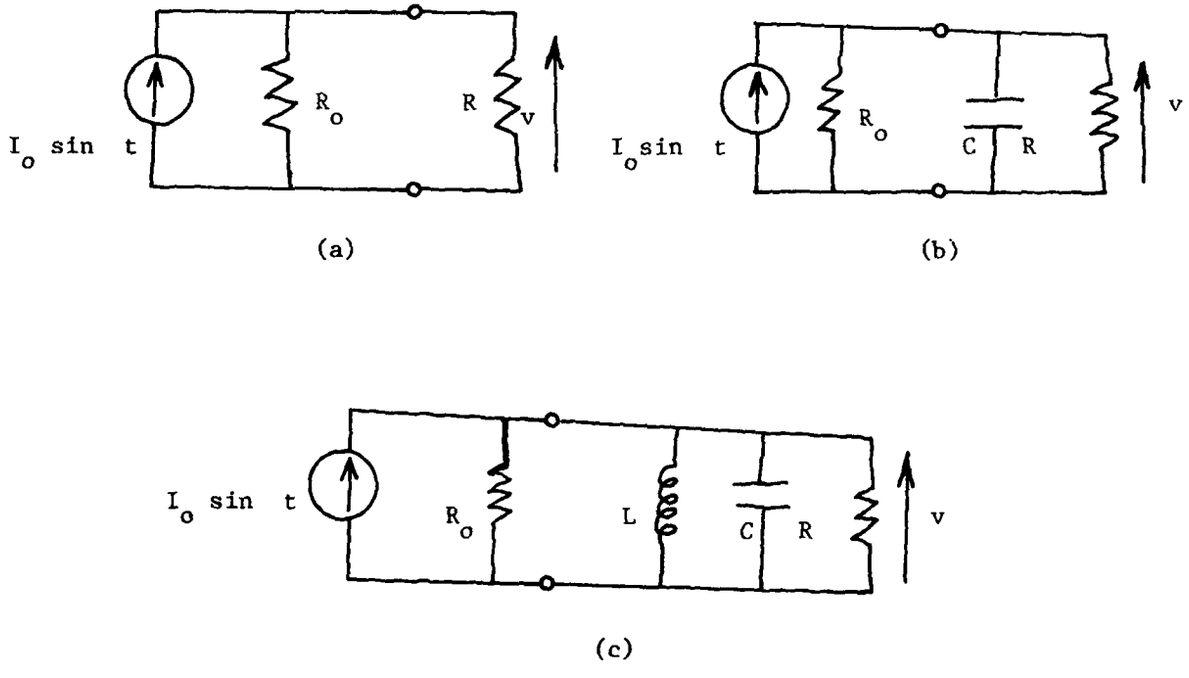

Figure 21. Circuits for Demonstrating "Instantaneous Impedance" Conecpt for Sinusoidal Excitation with Reactive Elements Present

that of the resistor alone and will indeed spend a significant fraction of time dewelling about the -1 value corresponding to the zero impedance interval of the capacitor, it is apparent that the power absorbed by the resistor should decrease. Just how much it decreases will depend upon the precise time-varying instantaneous impedance of the capacitor and hence upon the value of capacitance C and the frequency ω of the drive signal. Calculating the instantaneous power absorbed by the resistor when paralleled by a capcitor yields

$$p_R(t) = \frac{I_o^2 R_p^2}{R[1 + (\omega R_p C)^2]} \sin^2(\omega t - \omega R_p C) \tag{51}$$

which for $C > 0$ yields a decrease in amplitude of instantaneous power absorbed by the resistor. Time average power is

$$P_{avg} = R_p^2 I_o^2 / 2R[1 + (\omega R_p C)^2] \tag{52}$$

which again shows the anticipated decrease in power absorbed caused by paralleling the resistor with the instantaneous impedance of the capacitor.

The important point of the preceeding discussion is our ability to use time-varying reflection coefficient to predict <u>decreases</u> or <u>increases</u> in power (or energy) absorbed in an element as a result of adding some new element to the circuit or of increasing the input signal level. This technique is obviously a very powerful tool where bounds or limits on power (or energy) are required.

As a further indication of the power of this "way of thinking" about circuits, consider the 3 elements in parallel as shown in Figure 21c. Here we have added both L and C elements in shunt with the resistor. The instantaneous impedances of both the capacitor and inductor are time-varying. The formal relationship for the capacitor was given above. For the inductor the instantaneous impedance is

$$Z_L(t) = L\frac{di_L/dt}{i_L} = \frac{V_L}{\frac{1}{L}\int V_L dt} = \frac{V_L}{i_L} \tag{53}$$

For sinusoidal input signal the instantaneous impedance of the inductor varies from infinite to zero each quarter cycle and is given by

$$Z_L(t)\Big|_{\sin \omega t} = \omega L \cot \omega t \tag{54}$$

Thus, in Figure 21c the constant instantaneous impedance of the resistor R is now paralleled by a pair of time-varying instantaneous impedances one of which varies from open to short and the other from short to open over each quarter cycle of the sinusoidal signal. The net result is that the instantaneous reflection coefficient of the combination deviates from the value for the resistor alone, and for every case except one, the power absorbed by the resistor is decreased by the presence of L and C in parallel. The decrease in power absorbed is due to the fact that the instantaneous reflection coefficient of the combination "dwells" a significant fraction of time about the high reflection values produced by the reactive elements over a portion of each quarter cycle. Instantaneous power absorbed by the resistor is

$$p_R(t) = \frac{I_o^2 R_p^2}{R\left[1 + \left(\omega R_p C - \frac{R_p}{\omega L}\right)^2\right]} \sin^2\left[\omega t - \left(\omega R_p C - \frac{R_p}{\omega L}\right)\right] \tag{55}$$

which is less than the power absorbed by the resistor alone for all cases except the case where

$$\omega^2 = \frac{1}{LC}$$

which is the situation we normally call resonance. From the point of view of instantaneous impedance and reflection coefficient, resonance occurs when <u>two time-varying</u> instantaneous impedances combine in such fashion as to produce a <u>resultant constant</u> instantaneous impedance. Time average power absorbed is

$$P_{avg} = \frac{R_p^2 I_o^2}{2R\left[1 + \left(\omega R_p C - \frac{R_p}{\omega L}\right)^2\right]} \qquad (56)$$

which again shows the anticipated decrease in power absorbed (except for the resonant case $\omega L = \frac{1}{\omega C}$) caused by the shunting effect of the strongly varying instantaneous impedances of the capacitor and inductor. Note clearly that it is the fraction of time that the resultant instantaneous reflection coefficient "dwells" near the maximum absorbing point that determines the power absorbed.

The above discussion and examples introduce the concepts of instantaneous impedance and reflection coefficient and apply them, in combination with fractional time calculations, for predictive extrapolation of absorbed power. The concepts are exceptionally general and may be applied with all types of elements, linear and nonlinear, active and passive. While it requires some time to become accustomed to thinking in these rather unorthodox terms, the approach seems promising for general purpose analysis of a number of EMC problems. This discussion represents only the beginning.

7.0 CONCLUSIONS

A new technique suitable for time-domain analysis of a very general class of lumped/distributed networks is introduced. The technique is useful in a wide range of EMC problems. In this report the basic procedure is described and illustrated with examples. Time-domain models of transmission lines and other structures can also be determined using the analysis technique. Such models are useful in existing CAD programs such as SCEPTRE and SPICE. This feature is illustrated by generating an exceptionally simple model for lossless transmission lines. Finally, a novel concept using time-varying reflection coefficients is introduced.

REFERENCES

1. J. L. Allen, "Analysis of Lumped-Distributed Networks," MTT Transactions, November 1979.

2. Bowers, J. C. and S. R. Sedore, SCEPTRE: A Computer Program for Circuit and Systems Analysis, Prentice-Hall, Inc., Englewood Cliffs, New Jersey, 1971.

3. Nagel, L. W., "SPICE2: A Computer Program to Simulate Semiconductor Circuits," Electronics Research Laboratory, University of California (Berkeley), Memorandum No. ERL-M520, May, 1975.

4. Silverberg, M. and O. Wing, "Time Domain Computer Solutions for Networks Containing Lumped Nonlinear Elements," IEEE Trans. Circuit Theory, September 1968, pp. 292-294.

5. Getsinger, W. J., "Analysis of Certain Transmission-Line Networks in the Time Domain," IRE Trans. MTT, May 1960, pp. 301 309.

6. Ross, G. F., "The Transient Analysis of Certain TEM Mode Four-Port Networks," IEEE Trans. MTT, NOvember 1966, pp. 528-542.

7. Stepanishen, P. R., "Transient Analysis of Lumped and Distributed Parameter Systems Using an Approximate Z-Transform Technique," J. Acoust. Soc. Am., Vol. 52, # 1 (Part 2), July 1972, pp. 270-282.

8. Liou, M. L., "A Novel Method of Evaluating Transient Response," Proc. IEEE, Vol. 54, January 1966, pp. 20-23.

9. Ho, I. T. and S. K. Mullick, "Analysis of Transmission Lines on Integrated-Circuit Chips," IEEE J. of Solid-State Circuits, December 1976, pp. 201-208.

10. Lonngren, K. E., et al., "Self-Similar Solution of Distributed Linear and Nonlinear Networks," IEEE Trans. CAS, November 1975, pp. 882-886.

11. Rabbat, N. B., "Efficient Computation of the Transient Response of Lumped-Distributed Linear Active Networks," IEEE Trans. CAS, August 1975, pp. 666-670.

12. Linner, L. J. Peter, "Time Domain Analysis of Commensurate Distributed-Line Networks," IEEE Trans. CAS, April 1975, pp. 334-343.

13. Calahan, D. A., Computer-Aided Network Design (Revised Edition), McGraw-Hill, Inc. (1972), pp. 246-249.

14. Branin, F. H., Jr., "Transient Analysis of Lossless Transmission Lines," Proc. IEEE, Vol. 55, November 1967, pp. 2012-2013.

15. Liu, Y. K., "Transient Analysis of TEM Transmission Lines," Proc. IEEE, Vol. 52, June 1968, pp. 1090-1092.

16. Fray, W. and P. Althammer, "The Calculation of Electromagnetic Transients on Lines by Means of a Digital Computer," Brown Boveri Review, Vol. 48, pp. 344-355, 1961.

17. Ameniya, H., "Time-Domain Analysis of Multiple Parallel Transmission Lines," RCA Review, June 1967, pp. 241-276.

18. Chang, Fung-Yuel, "Transient Analysis of Lossless Coupled Transmission Lines in Nonhomogeneous Dielectric Medium," IEEE Trans. MTT, September 1970, pp. 616-626.

19. Weinberg, L., Network Analysis and Synthesis, McGraw-Hill, Inc. (1962).

20. Kron, G., Tensors for Circuits (2nd Edition), Dover Publications, Inc. (1942, 1959).

21. Chua, L. O. and Pen-Min Lin, Computer Aided Analysis of Electronic Circuits (Algorithms and Computational Techniques), Prentice-Hall, Inc. (1975).

MISSION
of
Rome Air Development Center

RADC plans and executes research, development, test and selected acquisition programs in support of Command, Control Communications and Intelligence (C^3I) activities. Technical and engineering support within areas of technical competence is provided to ESD Program Offices (POs) and other ESD elements. The principal technical mission areas are communications, electromagnetic guidance and control, surveillance of ground and aerospace objects, intelligence data collection and handling, information system technology, ionospheric propagation, solid state sciences, microwave physics and electronic reliability, maintainability and compatibility.